classified
urity Classification of this page

REPORT DOCUMENTATION PAGE

Report Security Classification: Unclassified	1b Restrictive Markings
Security Classification Authority	3 Distribution/Availability of Report Approved for public release; distribution is unlimited.
Declassification/Downgrading Schedule	
Performing Organization Report Number(s)	5 Monitoring Organization Report Number(s)
Name of Performing Organization aval Postgraduate School — 6b Office Symbol (if applicable) 31	7a Name of Monitoring Organization Naval Postgraduate School
Address (city, state, and ZIP code) onterey CA 93943-5000	7b Address (city, state, and ZIP code) Monterey CA 93943-5000
Name of Funding/Sponsoring Organization — 6b Office Symbol (if applicable)	9 Procurement Instrument Identification Number
ldress (city, state, and ZIP code)	10 Source of Funding Numbers Program Element No — Project No — Task No — Work Unit Accession No

Title (include security classification) THREE DIMENSIONAL FIBER-OPTIC LDV MEASUREMENTS IN THE ENDWALL EGION OF A LINEAR CASCADE OF CONTROLLED-DIFFUSION STATOR BLADES

Personal Author(s) David M. Dober

a Type of Report	13b Time Covered	14 Date of Report (year, month, day)	15 Page Count
aster's Thesis	From To	1993, March, 25	128

Supplementary Notation The views expressed in this thesis are those of the author and do not reflect the official policy or position the Department of Defense or the U.S. Government.

Cosati Codes			18 Subject Terms (continue on reverse if necessary and identify by block number)
eld	Group	Subgroup	Laser Doppler Velocimetry,LDV,Fiber-Optic LDV,Cascade Wind Tunnel,Controlled-Diffusion Blades,Endwall Region,Vortices,Secondary Flow

Abstract (continue on reverse if necessary and identify by block number)

Measurements were taken of the vortex system that results from the interaction between a stator blade tip nd the approaching endwall boundary layer in a linear cascade of controlled-diffusion compressor stator lades. Measurements were taken at Reynolds numbers based on stator blade chord of 240000 and 711000. otal pressure measurements were first conducted upstream and downstream of the controlled-diffusion stator lades. The approaching boundary layer was characterized and the location of the downstream vortices were pproximated. Upstream and downstream three-dimensional fiber-optic LDV surveys were then conducted to bserve the velocity profiles of the approaching boundary layer and to map the location and velocity haracteristics of the downstream vortex system. Results clearly show the effect that the overall secondary ow in the blade passage has on the location of the two oppositely rotating vortices. The downstream flow haracteristics were also shown to be periodic.

Distribution/Availability of Abstract X unclassified/unlimited __ same as report __ DTIC users	21 Abstract Security Classification Unclassified
a Name of Responsible Individual arth V. Hobson	22b Telephone (include Area Code) (408) 656-2888 — 22c Office Symbol Code AA/Hg

D FORM 1473,84 MAR — 83 APR edition may be used until exhausted — security classification of this page

All other editions are obsolete — Unclassified

Approved for public release; distribution is unlimited.

Three-Dimensional Fiber-Optic LDV Measurements in the Endwall Region of a Linear Cascade of Controlled-Diffusion Stator Blades

by

David Michael Dober
Lieutenant, United States Navy
B.S., United States Naval Academy, 1983

Submitted in partial fulfillment
of the requirements for the degree of

MASTER OF SCIENCE IN AERONAUTICAL ENGINEERING

from the

NAVAL POSTGRADUATE SCHOOL
March 1993

ABSTRACT

Measurements were taken of the vortex system that results from the interaction between a stator blade tip and the approaching endwall boundary layer in a linear cascade of controlled-diffusion compressor stator blades. Measurements were taken at Reynolds numbers based on stator blade chord of 240000 and 711000. Total pressure measurements were first conducted upstream and downstream of the controlled-diffusion stator blades. The approaching boundary layer was characterized and the downstream vortex locations were approximated. Upstream and downstream three-dimensional fiber-optic LDV surveys were then conducted to observe the velocity profiles of the approaching boundary layer and to map the location and velocity characteristics of the downstream vortex system. Results clearly show the effect that the overall secondary flow in the blade passage has on the location of the two oppositely rotating vortices. The downstream flow characteristics were also shown to be periodic.

TABLE OF CONTENTS

I. INTRODUCTION....................1

II. EXPERIMENTAL APPARATUS....................5

A. SUBSONIC LINEAR CASCADE....................5

B. INSTRUMENTATION AND DATA ACQUISITION....................5

III. EXPERIMENTAL PROCEDURES....................17

A. CASCADE TUNNEL SET-UP AND PNEUMATIC RAKE PROBE SURVEYS....................17

B. LDV SET-UP AND SYSTEM VALIDATION....................18

C. LDV SURVEYS....................27

D. LDV DATA PROCESSING....................30

IV. RESULTS AND DISCUSSION....................32

A. UPSTREAM PNEUMATIC RAKE PROBE DATA....................32

B. DOWNSTREAM PNEUMATIC RAKE PROBE DATA....................32

C. UPSTREAM LDV DATA WITH RE_C=240000....................38

D. DOWNSTREAM LDV DATA WITH RE_C=240000....................45

E. DOWNSTREAM LDV DATA WITH RE_C=711000....................51

V. CONCLUSIONS AND RECOMMENDATIONS....................61

APPENDIX A. PNEUMATIC RAKE PROBE SOFTWARE................64

A. INTRODUCTION..........................64

APPENDIX B. LDV DATA FOR RE_C=711000......................79

APPENDIX C. RAKE PROBE DATA TABULATION RE_C=240000........82

APPENDIX D. LDV SYSTEM COMPARISON........................112

REFERENCES..113

INITIAL DISTRIBUTION LIST...............................115

LIST OF FIGURES

Figure 1. Development of Vortical Flow Within Blade Passages....................4

Figure 2. NPS Cascade Wind Tunnel Test Facility..........6

Figure 3. Cascade Tunnel Cross Section...................7

Figure 4. Controlled-Diffusion Blade Geometry............8

Figure 5. Pneumatic Rake Probe Data Acquisition System..10

Figure 6. LDV System....................................11

Figure 7. Laser and Optics..............................12

Figure 8. Traverse Table and Power Supply...............16

Figure 9. LDV System Layout.............................19

Figure 10. Probe Orientation and Coordinate System.......23

Figure 11. Aligning Tool.................................24

Figure 12. Surveys Stations Between Blades Seven and Eight for LDV Measurements..........28

Figure 13. Histogram from FIND 3.5 Statistical Program...31

Figure 14. Upstream Pitchwise Pressure Distribution 6.0 Inches from the North Wall................33

Figure 15. Upstream Spanwise Pressure Distribution for Station 6....................33

Figure 16. Upstream Pitchwise Pressure Distribution 0.03125 Inches from the North Wall............34

Figure 17. Upstream Pitchwise Pressure Distribution 0.09375 Inches from the North Wall............34

Figure 18. Upstream Pitchwise Pressure Distribution 0.21875 Inches from the North Wall............35

Figure 19. Upstream Pitchwise Pressure Distribution 0.46875 Inches from the North Wall............35

Figure 20. Upstream Pitchwise Pressure Distribution 0.96875 Inches from the North Wall............36

Figure 21. Upstream Pitchwise Pressure Distribution 1.46875 Inches from the North Wall............36

Figure 22. Downstream Pitchwise Pressure Distribution 6.0 Inches from the North Wall................37

Figure 23. Downstream Pitchwise Pressure Distribution 2.0 Inches from the North Wall................39

Figure 24. Downstream Pitchwise Pressure Distribution 3.0 Inches from the North Wall................39

Figure 25. Inlet Pitchwise Survey of the Pitchwise Velocity 4.0 Inches from the Endwall at Station 1.................40

Figure 26. Inlet Pitchwise Survey of the Spanwise Velocity 4.0 Inches from the Endwall at Station 1.................40

Figure 27. Inlet Pitchwise Survey of the Axial Velocity 4.0 Inches from the Endwall at Station 1.................41

Figure 28. Inlet Pitchwise Survey of the Pitchwise Velocity 0.75 Inches from the Endwall at Station 1.................41

Figure 29. Inlet Pitchwise Survey of the Spanwise Velocity 0.75 Inches from the Endwall at Station 1.................42

Figure 30. Inlet Pitchwise Survey of the Axial Velocity 0.75 Inches from the Endwall at Station 1.................42

Figure 31. Inlet Pitchwise Survey of the Pitchwise Velocity 0.25 Inches from the Endwall at Station 1.................43

Figure 32. Inlet Pitchwise Survey of the Spanwise Velocity 0.25 Inches from the Endwall at Station 1.................43

Figure 33. Inlet Pitchwise Survey of the Axial Velocity 0.25 Inches from the Endwall at Station 1.................44

Figure 34. Downstream Pitchwise Survey of the Pitchwise Velocity 0.75 Inches from the Endwall at Station 19.........46

Figure 35. Downstream Pitchwise Survey of the Pitchwise Velocity 0.5 Inches from the Endwall at Station 19.........46

Figure 36. Downstream Pitchwise Survey of the Spanwise Velocity 0.75 Inches from the Endwall at Station 19.........47

Figure 37. Secondary Flow Due to Case Wall Boundary Layers.....................47

Figure 38. Velocity Field in the Exit Plane at Station 19......................48

Figure 39. Z-Component of Vorticity in the Exit Plane at Station 19..................50

Figure 40. Downstream Pitchwise Surveys of the Pitchwise Velocity at Various Distances from the Endwall at Station 19......52

Figure 41. Standard Deviation of the Pitchwise Velocity at Various Distances from the Endwall at Station 19......53

Figure 42. Downstream Pitchwise Surveys of the Spanwise Velocity at Various Distances from the Endwall at Station 19......53

Figure 43. Standard Deviation of the Spanwise Velocity at Various Distances from the Endwall at Station 19......54

Figure 44. Downstream Pitchwise Surveys of the Axial Velocity at Various Distances from the Endwall at Station 19......54

Figure 45. Standard Deviation of the Axial Velocity at Various Distances from the Endwall at Station 19......55

Figure 46. Velocity Field in the Exit Plane at Station 19......................57

Figure 47. Z-Component of Vorticity in the Exit Plane at Station 19..................58

Figure 48. Downstream Pitchwise Surveys of the Axial Velocity at Various Distances from the Endwall at Station 19......59

Figure A1. Keyboard Diagram................................66

Figure A2. Example of the Output from the Spanwise Normalization Option.............73

Figure A3. Example of the Output from the Pitchwise Normalization Option............75

Figure A4. Example of Static Pressure Output.............76

Figure A5. Example of Surface Plot Output................78

LIST OF SYMBOLS

C_p	coefficient of pressure
u	pitchwise velocity component
v	spanwise velocity component

ACKNOWLEDGMENTS

I would like to thank Prof. Hobson for the guidance he has provided to me throughout this endeavor and for his patience when conducting long-winded explanations. His enthusiasm has made this a truly memorable and rewarding experience. Thanks also to Rick Still and Thad Best for their technical support and friendship. Special thanks to my wife, Mary Beth, without her undying support and infinite patience none of my accomplishments would ever be attainable. This work is dedicated to my two daughters, Meighan and Emily.

I. INTRODUCTION

The trend of axial machine design is toward higher blade loadings and lower aspect ratios which places more emphasis on endwall effects and tip clearance losses [Ref. 1]. Endwall effects and tip clearance losses are results of secondary flows around blade tips and within blade passages. Secondary flows are always present in any axial machine in both rotor and stator sections. Computational modelling of these complex three-dimensional flows has proven to be very difficult. There are a number of computational fluid dynamic (CFD) programs available that model three-dimensional turbomachinery flows and attempts to predict the losses induced by these flows have had limited success. A thorough analysis of the secondary flows must be completed prior to attempting to refine the present CFD codes for better loss prediction.

Secondary flows are highly complex in nature and require a full three-dimensional analysis to be fully understood. This analysis requires full three-dimensional measurement of the flow field. Data on these flow fields be can acquired either intrusively or non-intrusively. The two major methods for acquiring flow field data intrusively are hot wires and pneumatic probes. Both measuring instruments are able to acquire extremely accurate data but require extensive calibration. Furthermore, both instruments will display some

sort of flow field interference that will become more significant as the distance from the instrument to a solid surface decreases. Pneumatic probes also have limited utility in very unsteady flows. One of the primary non-intrusive measurement techniques is laser Doppler velocimetry (LDV), which will be the focus of this work.

The LDV technique has been used for a number of years now. A little over a decade ago the first results of using LDV for three-dimensional flow field measurements were published. One of the first attempts used a one-component LDV system that rotated through three different positions to map the three-dimensional flow field downstream of a set of airfoils in a non-rectilinear cascade [Ref. 2].

Only within the last six or seven years has three-dimensional LDV been used specifically for turbomachinery applications. A two-component LDV system that is able to move in all three dimensions has been used to measure the three-dimensional flow field in a radial-inflow turbine scroll [Ref. 3]. A three-component LDV system has been used with off-axis backscatter to measure the three-dimensional flow field in the rotor blade passage of an axial-flow compressor [Ref. 4]. Most recently a three-component LDV system was used to measure the unsteady flow field in the rotor of a radial-inflow turbine [Ref. 5].

This work will focus on the secondary flow that exists downstream of a set of controlled-diffusion stator blades in

a linear cascade. A three-component fiber-optic LDV system was used to map the flow field. The downstream vortices result from the interaction between the endwall boundary layer and the stator blade tips, as illustrated in Figure 1. There is no tip clearance gap associated with this linear cascade. The endwall boundary layer flow approaching the leading edge of each blade in the cascade separates and rolls up into the familiar horse-shoe vortex found around all blunt obstacles standing out of a shear flow. The leg of the vortex on the suction side is moved spanwise away from the endwall by the secondary flow in the passage. The leg of the vortex on the pressure side is convected across the passage to join the suction surface of an adjacent blade so that the endwall suction surface corner has two vortices rotating in opposite directions [Ref. 6]. Measurements were made upstream and downstream of the controlled-diffusion blades using both a 20 hole pneumatic rake probe and the three-component fiber-optic LDV system. Measurements were made at two different Reynolds numbers, the low Reynolds number having no inlet boundary layer control and the high Reynolds number with upstream boundary layer control by using suction slots.

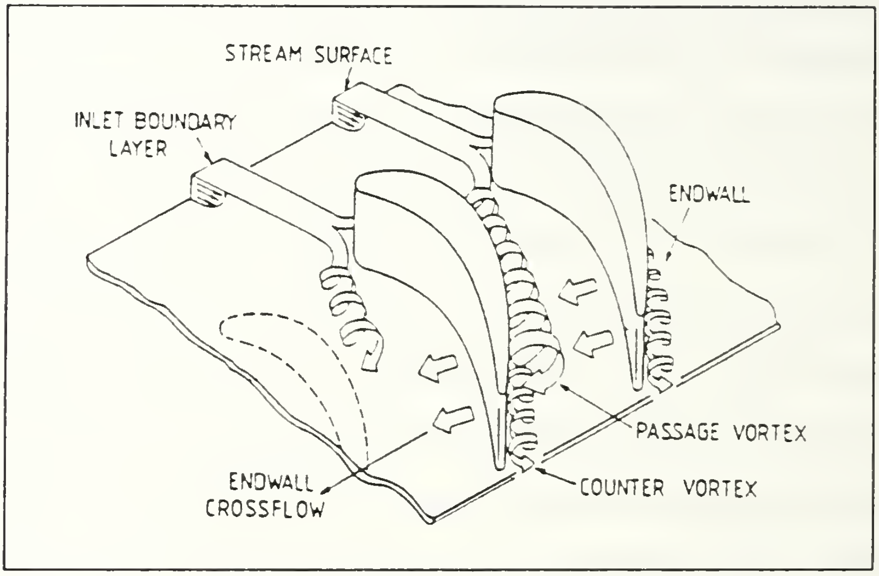

Figure 1. Development of Vortical Flow Within Blade Passages

II. EXPERIMENTAL APPARATUS

A. SUBSONIC LINEAR CASCADE

The NPS cascade wind tunnel test facility is shown is Figure 2. A thorough description of the facility, test section and controlled-diffusion blading is contained in Reference 7 [Ref. 7]. Figure 3 is a cross section of the cascade tunnel and shows the position where seed particles were introduced in the tunnel for LDV measurements. Figure 4 shows the controlled-diffusion blade profile. There were 20 blades in the test section.

B. INSTRUMENTATION AND DATA ACQUISITION

1. Pneumatic Probe Instrumentation and Data Acquisition

A 20 hole pneumatic rake probe was utilized for total pressure data surveys. There were 17 total pressure ports, one static pressure port and two yaw ports on the probe. For details on the probe construction and calibration see Webber's March 1993 master's thesis [Ref. 8].

Data acquisition and processing was done using an existing Hewlett Packard system. The programs for the system were developed by Classick in 1989, who also fully described the hardware [Ref. 9]. The only change made for this work was the addition of the 20 hole pneumatic rake probe to Scanivalve

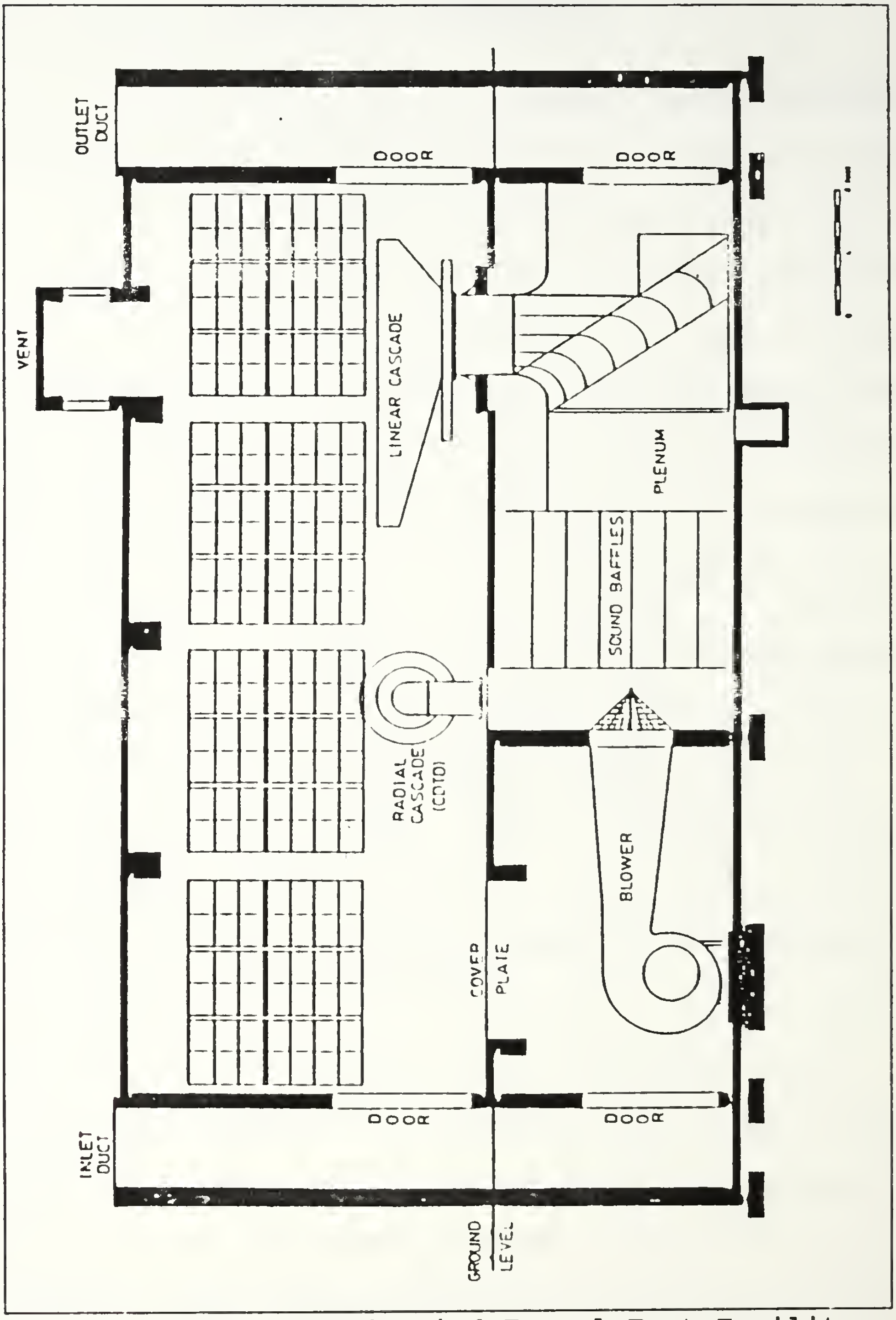

Figure 2. NPS Cascade Wind Tunnel Test Facility

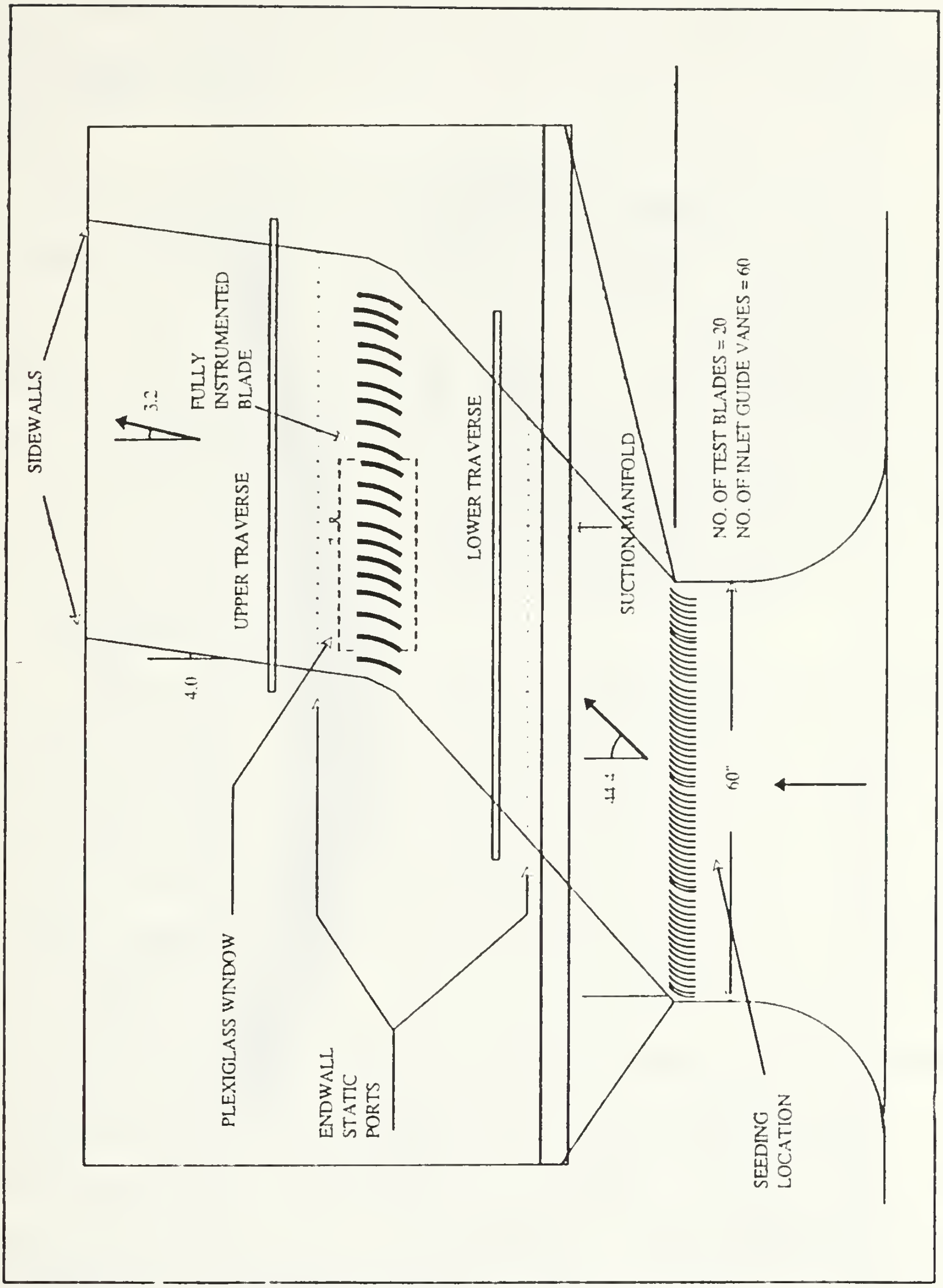

Figure 3. Cascade Tunnel Cross Section

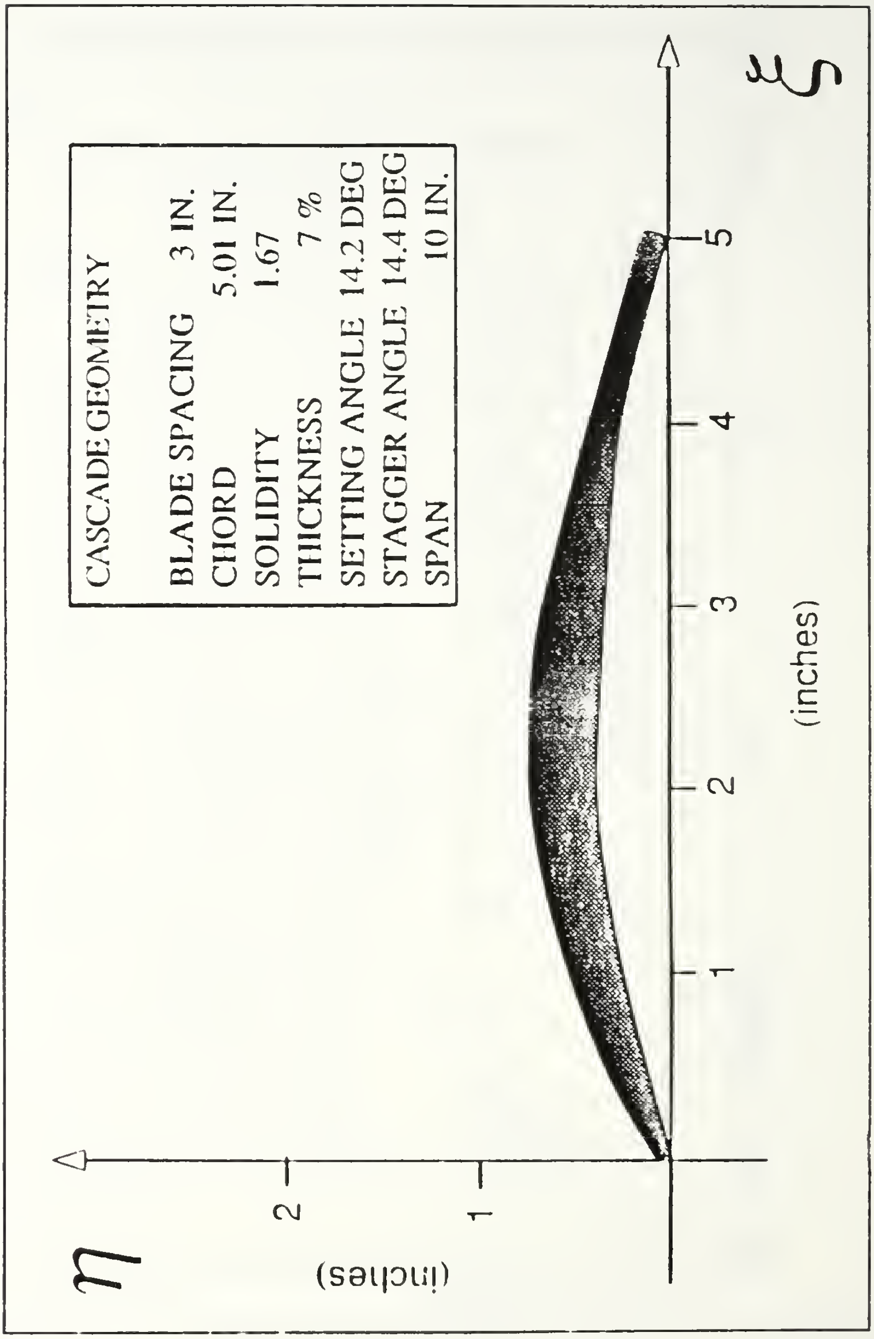

Figure 4. Controlled-Diffusion Blade Geometry

number 2 in the original system. Figure 5 shows a schematic of the data acquisition hardware. Classick's original ACQUIRE data acquisition program was modified for application in this work and the complete software modification is described in Appendix A.

2. LDV Instrumentation and Data Acquisition

The LDV system utilized for this work was a TSI three-component fiber-optic system. There were four major subsystems to this system: laser and optics, data acquisition system, traverse table and seeding. Figure 6 is a photograph of the LDV system. Figure 7 is a photograph of the laser and optics.

a. Laser and Optics

A five Watt Lexel model 95 Argon ion laser was used as the laser source. The laser was operated in the multi-line mode and was aligned to fire directly into a multicolor beam separator. The multicolor beam separator, a TSI model 9201 Colorburst, takes the beam from the laser source and splits it into two separate beams. One beam is passed through a Bragg cell to allow frequency shifting on that beam. Both beams are then passed through a prism for color separation. The Colorburst produces three pairs of beams: green (514.0 nm), blue (488.0 nm) and violet (476.5 nm). The six beams are then reflected vertically into six fiber-optic couplers. A coupler will align the laser beam onto the center of a

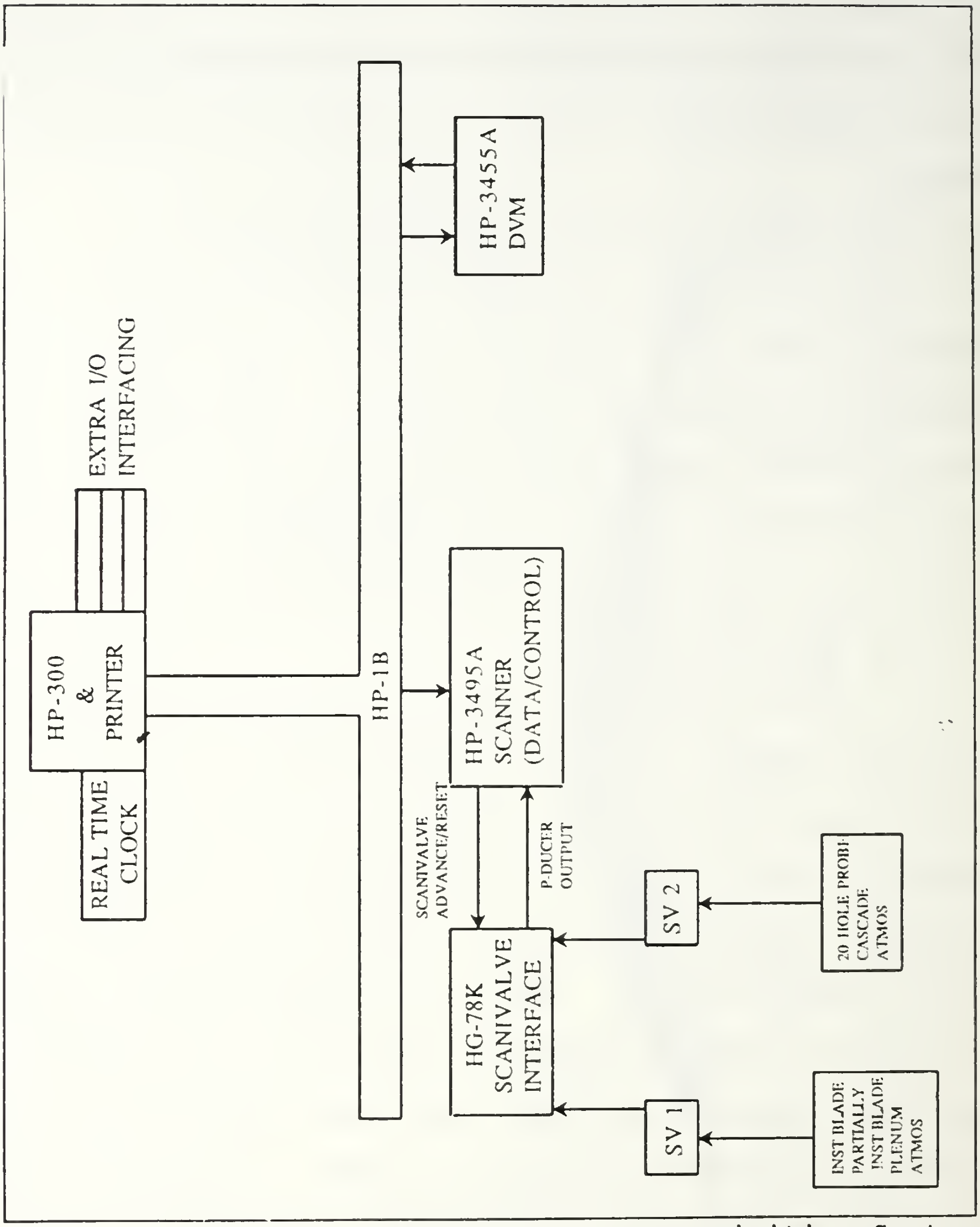

Figure 5. Pneumatic Rake Probe Data Acquisition System

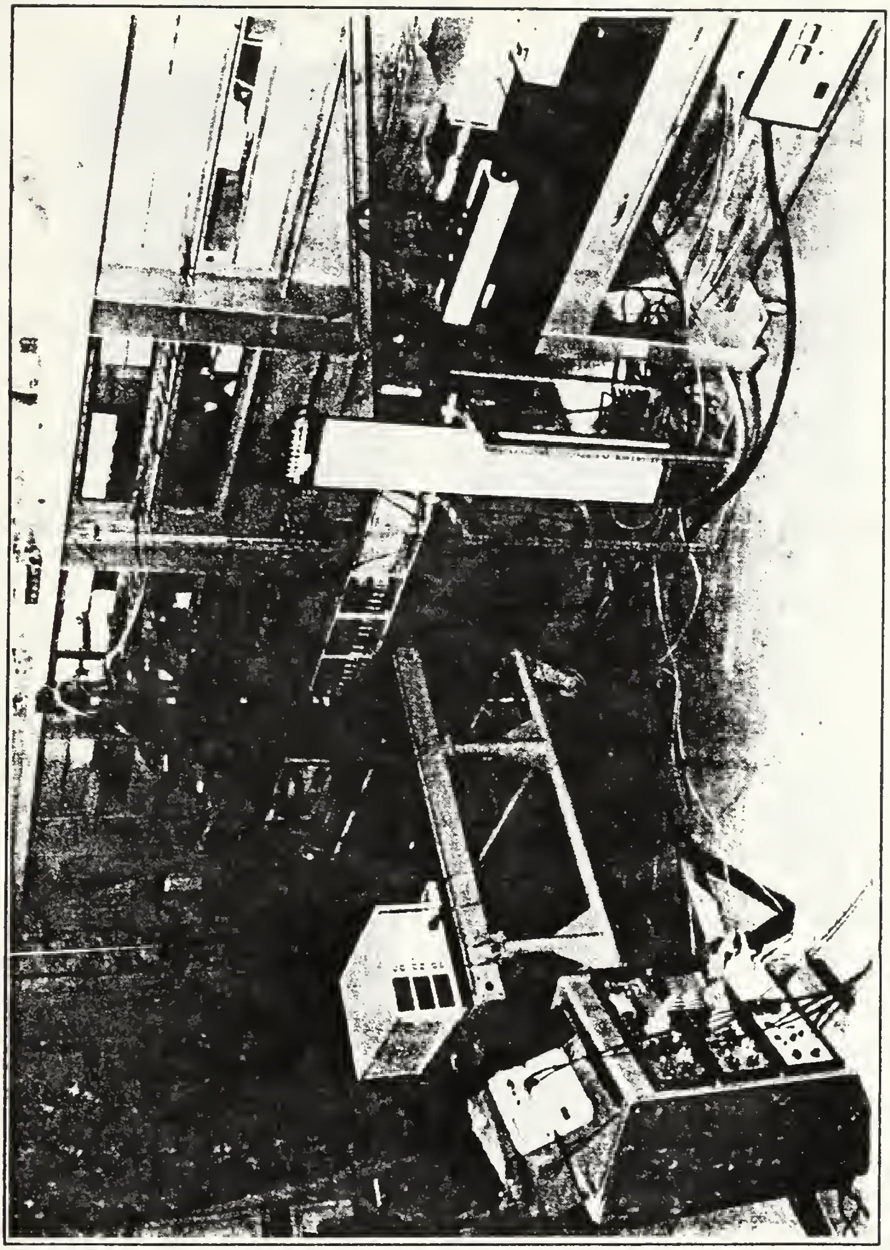

Figure 6. LDV System

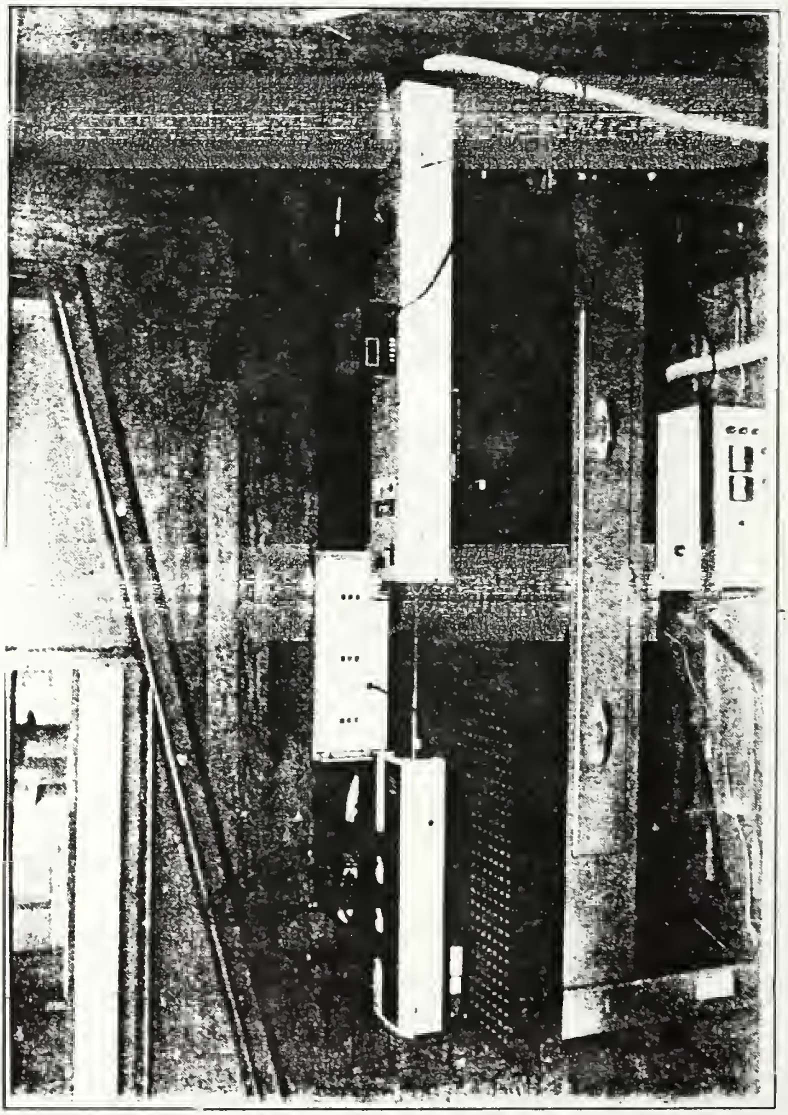

Figure 7. Laser and Optics

transmitting fiber-optic line and focus the beam waist at the end of the fiber. The polarization of the six individual laser beams is completed within the Colorburst and they are polarized in the same direction. The transmitting fiber-optic lines are formed into an elliptical shape by an extrusion process at the time of manufacture. The polarization direction of the laser beam at the coupler exit must be aligned with the semi-major axis of the transmitting fiber-optic line for polarization preservation in the fiber-optic line. If it is not aligned with the semi-major axis then the polarization direction will change all the way along the transmitting fiber-optic line. There are six transmitting fiber-optic lines in the system. Four are for the two-component probe and two are for the one-component probe. Final polarization direction of each beam is set by the manufacturer by twisting the transmitting fiber-optic lines and gluing them into place. Each time the system is disassembled, transported and reassembled the polarization directions should be checked at the exit of the couplers and at the exit of the probes. The probes separate the beams by 50 mm and the final lens focuses the beams of similar colors onto a point at a focal distance of 349.8 mm. The probes are 83 mm in diameter.

b. Data Acquisition

Scattered light from the seed particles is collected by each 83 mm probe and fed back to a TSI model 9230 Colorlink via a return fiber-optic line. The feedback signal from the one-component probe is sent through a violet filter and then to a photomultiplier tube within the Colorlink. The feedback signal from the two-component probe has the green beam separated from it, with a refracting mirror, and that green light goes through a green filter to a photomultiplier tube. The un-refracted beam is directed through a blue filter to a third photomultiplier tube. The Colorlink contains all the components necessary to collect the scattered light and complete the downmixing. The downmixed signals from the Colorlink are then sent to three separate TSI model 1990C counter-type signal processors. The counters will determine which signals are valid according to the settings that the user has chosen. The signals from the counters are fed to an IBM PC-AT via an MI-990 multichannel interface. TSI's FIND version 3.5 was installed on the IBM PC-AT and was used to process the Doppler signals.

c. Traverse Table

The two fiber-optic probes were mounted on an "I" beam attached to a traverse table that was capable of moving 600 mm in all three directions. The traverse table power supply, with digital readout, was controlled by the FIND 3.5

software via an RS-232 connection or it could be controlled manually. Figure 8 is a photograph of the traverse table and its power supply.

d. Seeding

One of the most critical issues in making LDV measurements is particle seeding. The selection of seeding material and the location where the seeding particles are injected into the flow are critical. The seeding particles must be the correct size, usually about one μm., in order to follow the flow properly, and must be able to scatter the light from the incident laser beam [Ref. 10]. Seeding location determines the area downstream in the test section that will contain enough seed particles to produce a sufficient data rate for data acquisition. The seeding source, which is usually a wand, must be located far enough upstream so that any flow field interference caused by the wand has time to mix out before the flow enters the test section.

Olive oil was used as the seeding material for the present LDV measurements. The seed particle generator was the same one that Elazar used [Ref. 11]. The average particle size from the particle generator was 0.9 μm with a standard deviation of 0.45 μm. Seeding material was injected into the flow upstream of the inlet guide vanes as shown in Figure 3.

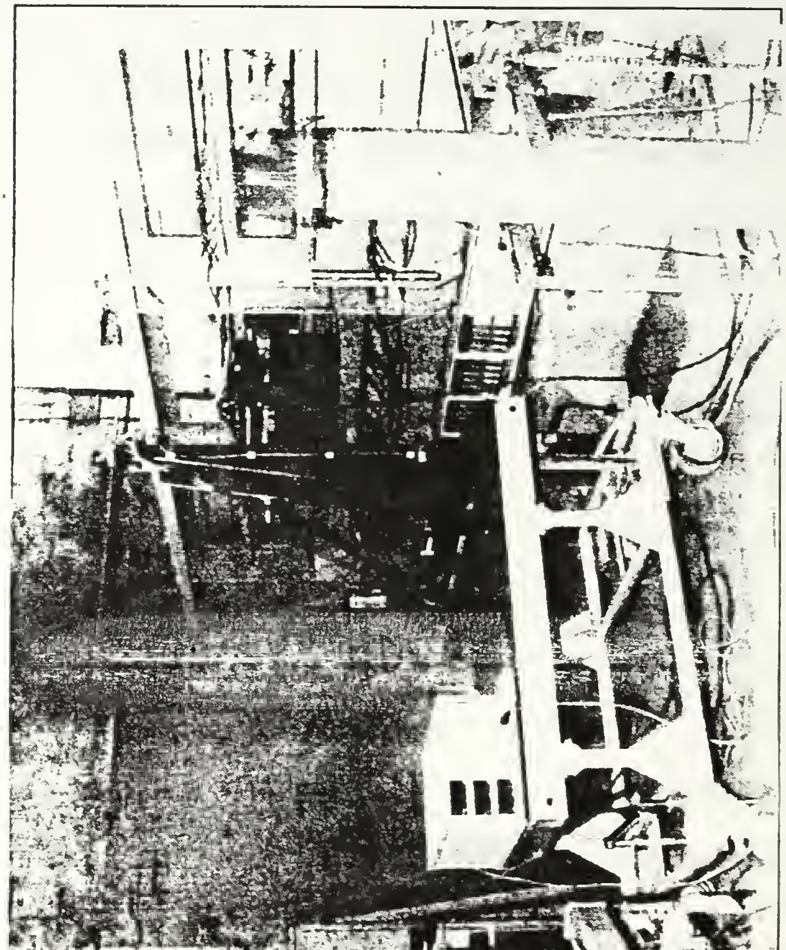

Figure 8. Traverse Table and Power Supply

III. EXPERIMENTAL PROCEDURES

A. CASCADE TUNNEL SET-UP AND PNEUMATIC RAKE PROBE SURVEYS

The inlet guide vanes on the cascade tunnel were set for an inlet flow angle, β_1, of 44.4 degrees as measured from the vertical. The tunnel was modified to include boundary layer suction slots located approximately 17 inches upstream of the leading edges of the controlled-diffusion blades. Webber described the details of the boundary layer suction slots and their performance [Ref. 8]. The first surveys were taken at the slowest speed of the tunnel with no boundary layer suction. The Reynolds number based on blade chord, Re_c, was 240000 for these surveys. This would allow the largest vortices to develop downstream of the controlled-diffusion blades. This was a test to determine whether the pneumatic rake probe and the LDV system could resolve the vortical flow prior to proceeding with higher inlet velocities. It was also an investigation into the periodicity of the downstream three-dimensional vortical flow in the endwall region. The valves to the suction plenum were completely closed and portions of the suction slots were taped off to prevent any flow interference with the developing boundary layer. Pneumatic rake probe surveys were conducted in a traverse slot located nine inches axially upstream of the controlled-diffusion

blades. The pneumatic rake probe spanned all ten inches of the cascade tunnel. Total pressure measurements were obtained every half inch for five inches. Total pressure gradients were analyzed to determine the size of the boundary layer approaching the controlled-diffusion blades. Total pressure measurements were also taken downstream of the controlled-diffusion blades in a traverse slot located 15 inches from the trailing edges of the blades. Measurements were obtained every quarter of an inch for 4.5 inches. Minimums in the total pressure readings were expected to denote the locations of the centers of the vortices at the downstream survey position. Periodicity in the total pressure profiles could be examined since the measurement length was larger than the blade spacing of three inches. A second set of pneumatic rake probe surveys was completed by Webber at a test section total pressure of 10.4 inches of water gauge and a boundary layer suction setting of 20 inches of water below atmosphere [Ref. 8]. These were the tunnel conditions used for the second set of downstream LDV measurements.

B. LDV SET-UP AND SYSTEM VALIDATION

The LDV components were set-up in accordance with the TSI instruction manuals. Figure 9 shows the connections between the system components. All components, except for the model 1990C processors, were capable of being controlled by the user at the computer keyboard. The TSI instruction manuals gave

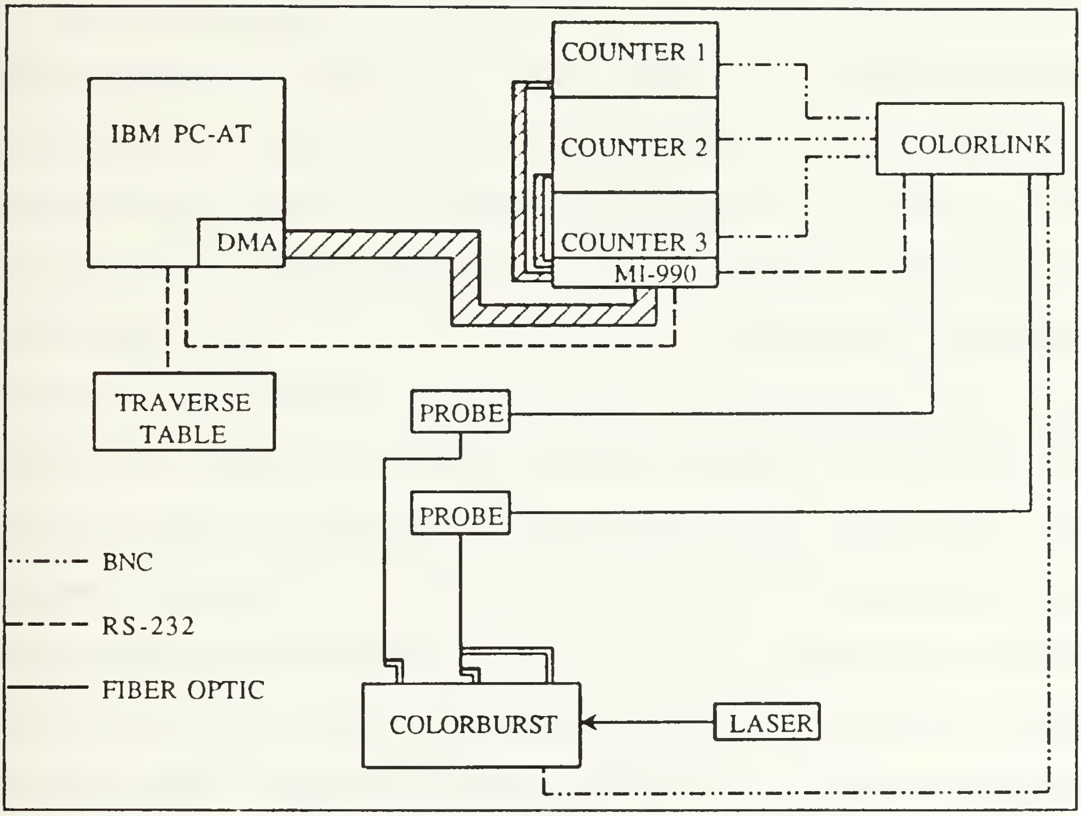

Figure 9. LDV System Layout

gave good step-by-step directions for system assembly but some system checks are included here for future operators. *Once the laser is aligned into the Colorburst the polarization directions must be checked at all six beam exits of the Colorburst to ensure proper operation of the Colorburst. During the focusing of the laser beams through the couplers on the fiber-optic ends, the total laser input power to the Colorburst must not exceed 500 mW. If the 500 mW input power is exceeded and the laser beam is striking the fiber-optic surface off center there is a possibility that the laser beam will melt the adhesive that holds the fiber-optic in place and the adhesive will form a coating over the end of the fiber-optic line. If this happens the system user will never attain the 50% transmitting fiber-optic power efficiency. The fiber-optic line ends must be polished to remedy this situation. The LDV system was operated here without a collimator between the laser and the Colorburst. Consequently the laser beam input to the Colorburst and the laser beams exiting from the Colorburst had relatively wide beam diameters. This made the final coupling procedure particularly difficult. When using a laser power meter during the final coupling process more than one peak power spot may be evident. Care must be taken to methodically determine which peak transmits the maximum power. At the beginning of the final coupler adjustments the difference in the peak power spots may be in the vicinity of a μW. The polarization out of the 83 mm probes must be*

the 83 mm probes must be checked to ensure that a proper fringe pattern will result from beam crossing. During the LDV system set-up it was discovered that one pair of beams was misaligned in polarization direction. There was a difference of about 40 degrees in polarization direction between the two beams. At this point polarization stability was checked. While observing the polarization direction from one of the beams out of the probe, the fiber-optic line at the coupler was perturbed. If the fiber was loose within the coupler the polarization direction would constantly change. No polarization direction change was observed and the probe was sent back to TSI for repair. The fringes themselves could not be observed because the Bragg cell could not be rotated out of the system, unlike in standard optic systems. If the probes are not used for an extended period of time, or are transported over a considerable distance, the focal length of the receiving fiber must be checked to ensure that it is focusing at the transmitting beam crossing. This process involves removing the back end of the probe and attaching a fiber-optic coupling line that allows the transmission of laser light from one of the couplers on the Colorburst, through the receiving fiber, and out of the probe. All laser beams exiting the probe must be directed through a microscopic objective to determine the beam crossing point and the receiving fiber focal length. This procedure was used to identify a bad receiving fiber in the two-component probe.

After the probes were mounted on the "I" beam of the traverse table, the beam crossing had to be checked. For this work, the probes were pointed 30 degrees from the perpendicular to the window. Figure 10 shows the probe orientation and the coordinate system used for the experiment. *To check beam crossing the microscopic objective must be used. Turn off the violet beams and fix all the adjustments on the two-component probe. Project the beams from the two-component probe into the microscopic objective and move the traverse table until the beam crossing point of the four beams is found. Turn off the green beams and turn on the violet beams. Use the adjustments on the one-component probe mount to adjust the focal point of the violet beams, and also to adjust the beam crossing point so that it overlaps the beam crossing point of the blue beams. A minimum of 80% overlap is required for data acquisition in the coincidence mode. Turn the green beams back on. The last step prior to commencing data acquisition is establishing the experimental coordinate system. Once the test section window is flush with the cascade tunnel walls, hang the aligning tool between blades seven and eight and ensure that it is up against the back of the test section window. Figure 11 is a drawing of the alignment tool that Elazar had built [Ref. 11]. The second central hole from the top was modified to allow alignment of the probe volume from probes that are mounted 30 degrees from the perpendicular to*

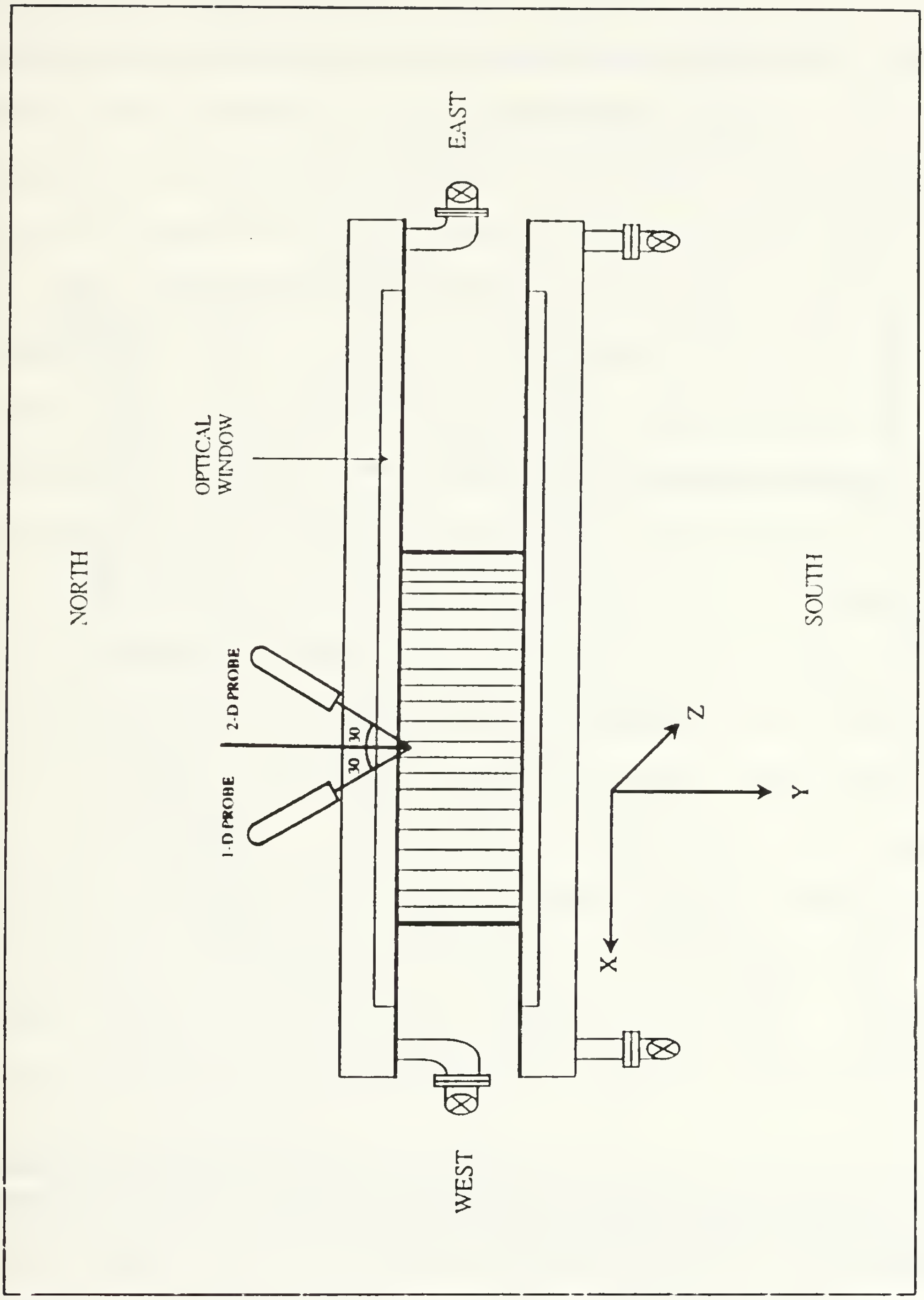

Figure 10. Probe Orientation and Coordinate System

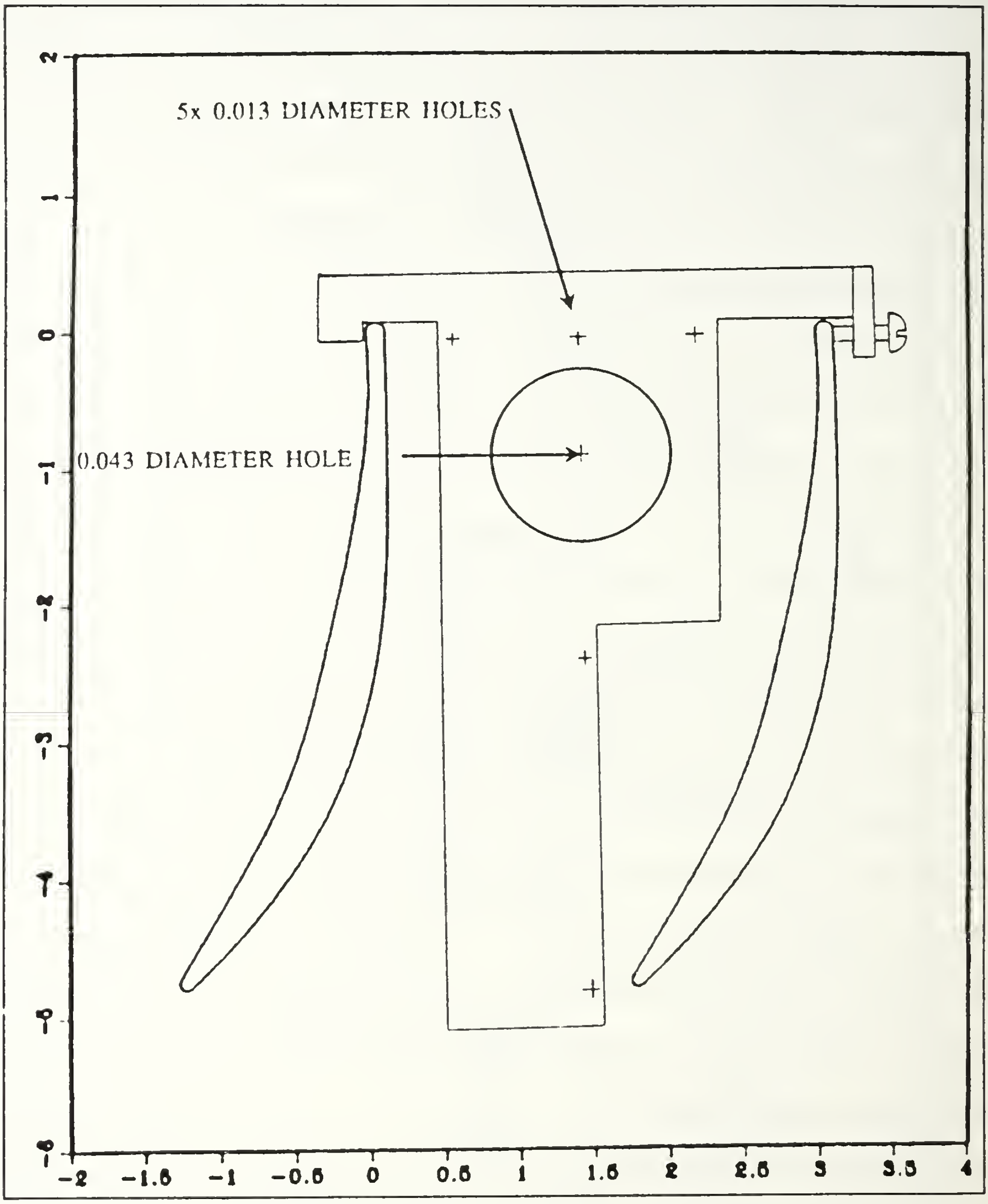

Figure 11. Aligning Tool

the test section window. Use manual traverse control to align the probe volume at the pin hole and push all three relative home buttons on the traverse power supply.

Turn the local traverse control off and establish computer control of the traverse table. Move the table to: x=-38.1 mm, y=-31.8 mm and z=21.996 mm. This moves the measurement volume to the center of the trailing edge of blade seven. Now select the relative home option on all three axes in the traverse table menu of FIND 3.5. This will zero out the distance indicators and establish the tunnel origin. When conducting surveys close to the test section window, the window will require cleaning about every two surveys. After window cleaning, the following items need to be completed prior to recommencing data acquisition: refine the focus of the Colorburst output beams on the transmitting fiber-optic lines and recheck the beam crossing of the two probes and adjust if necessary. When the window does not require cleaning between surveys, move the measurement volume to the first point of the next survey and select the real time histogram option on the data acquisition menu. This is required to check the coincidence data rate to ensure that the beam crossing is adequate.

Control of the traverse table has one anomaly that needs to be mentioned. Once computer control of the traverse table is accomplished a switch to manual traverse control cannot be accomplished simply by pressing the local control button. The

power switch on the back of the traverse table power supply needs to be cycled to establish manual traverse control. Once the power switch is cycled, all three distance indicators on the power supply become zero. In order to preserve the measurement volume alignment, use computer control to move the traverse table to the origin prior to cycling the power switch to establish manual control. Computer control can be established anytime the local control button on the traverse table power supply is off.

System validation was completed by a comparison between the fiber-optic LDV system and a standard optic system that was already installed on the cascade tunnel, as described by Murray [Ref. 12]. The fiber-optic probes were mounted perpendicular to the window of the test section and data were collected from each probe focussed at the same point in the flow field upstream of the controlled-diffusion blades. The standard optic system was also used to collect data at the same point in the flow field. Both fiber-optic probes agreed with the standard optic system to within five percent. The standard optic system was removed and the traverse table for the fiber-optic system was installed. The probes were mounted on the traverse table "I" beam pointing 30 degrees off the perpendicular to the test section window. The optics window in FIND 3.5 contained an on-axis velocity computation mode. Two pairs of beams could be used to measure velocity components that were in the same plane but not necessarily

normal to each other. The angular settings for off-axis measurements through the window were set in this mode. The angular settings were used by the software, in a coordinate transformation, to determine the magnitudes of the two perpendicular velocity components in the plane. There was also a rotation and tilt feature so the software coordinate system could be matched to the experimental coordinate system. Settings for this work in the on-axis computation mode were +30 degrees for the two-component probe and -30 degrees for the one component probe. The software coordinate system was rotated +90 degrees to match the experimental coordinate system. The same point in the flow field was used to compare velocity computations in the on-axis mode. Results were within two percent of the measurements that were conducted perpendicular to the test section window.

C. LDV SURVEYS

LDV surveys were conducted both upstream and downstream of the controlled-diffusion blades. The origin of the test section coordinate system was set at the center of the trailing edge radius of blade number seven. Elazar developed standard LDV survey stations based on the y coordinate [Ref. 11]. Figure 12 shows the LDV surveys stations. Station 1 was used for the upstream surveys and station 19 was used for the downstream surveys.

		1	2	3	4	5	6	7	8	
		-6.292	-4.792	-4.542	-4.292	-4.042	-3.792	-3.292	-2.792	
9	10	11	12	13	14	15	16	17	18	19
-2.292	-1.792	-1.292	-0.792	-0.5	-0.25	0.0	0.262	0.362	0.678	1.062

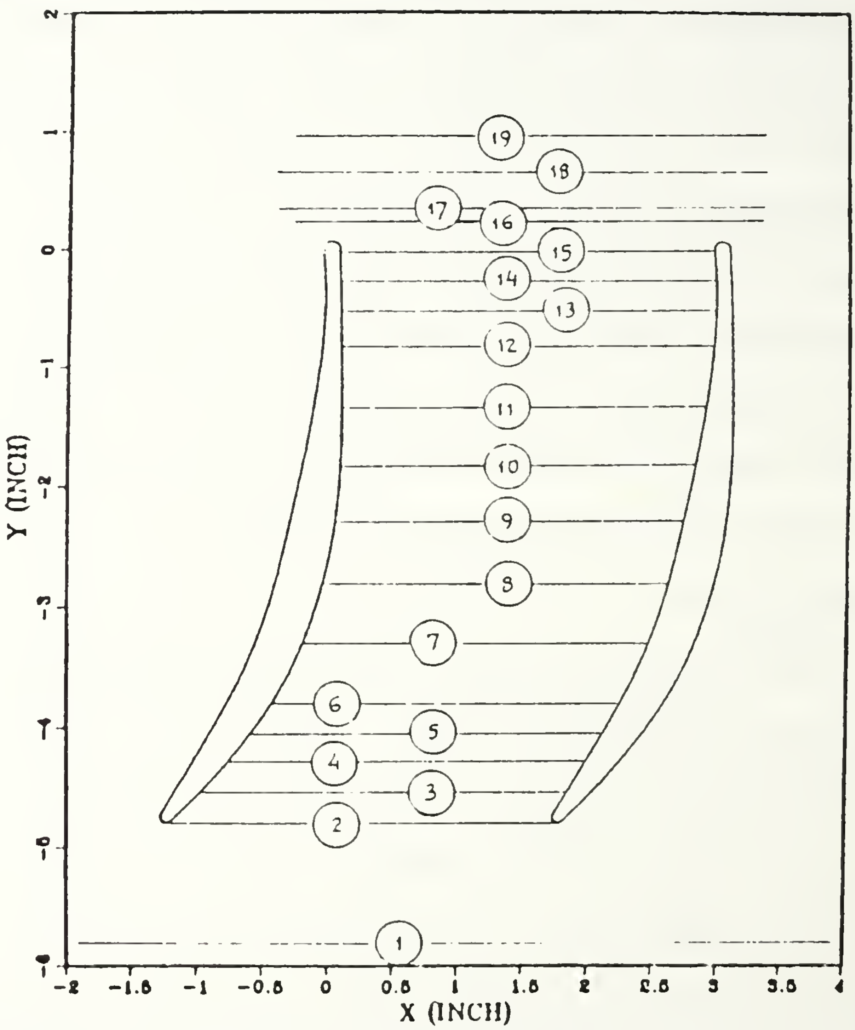

Figure 12. Surveys Stations Between Blades Seven and Eight for LDV Measurements

The first set of LDV surveys were taken at a Re_c of 240000. The test section total pressure, as read from a Prandtl probe, was 1.20 inches of water gauge. Upstream surveys were conducted at station 1 every half inch in the pitchwise direction with x ranging from minus three to two inches. The y coordinates for the pitchwise surveys were: 4.0, 2.5, 1.5, 0.75 and 0.25 inches. Downstream surveys were taken at station 19 every quarter of an inch in the pitchwise direction with x ranging from minus one to four inches. The y coordinates for the downstream surveys were: 4.0, 2.5, 2.0, 1.5, 1.125, 0.75, 0.50 and 0.25 inches. Data were acquired in the coincidence mode and frequency shifting of 2 Mhz was required for the downstream surveys on the green and violet beams which were measuring velocity components in the horizontal plane.

A second set of LDV surveys was completed at a Re_c of 711000. The test section total pressure for these surveys was held constant at 10.4 inches of water gauge and a boundary layer suction level of 20 inches was used. Upstream rake probe surveys of this flow were completed by Webber [Ref. 8]. The matrix of data acquisition points was much finer on these surveys in an attempt to map a potentially smaller vortex due to the endwall boundary layer removal. Surveys were completed at station 19 with x ranging from minus one to two inches at increments of 0.15 inches. The y coordinates for the pitchwise surveys were: 2.00, 1.67, 1.33, 1.00, 0.80, 0.60,

0.40 and 0.25 inches. Frequency shifting of 5 Mhz was required on the green and violet beams. The frequency shifting had to be increased to 10 Mhz on the green beams on the survey closest to the test section window.

D. LDV DATA PROCESSING

The statistical analysis of the LDV data was completed in the statistics program in FIND 3.5. None of the data histograms were manually edited and averaging was performed over 1024 data points at each measurement location. Figure 13 is an example of a histogram that was produced from the LDV raw data by the statistics program in FIND 3.5. The data at the Re_c of 711000 were processed using the refinement bounds set at plus or minus two standard deviations. This means that all the statistics for these surveys are based on data that are within two standard deviations of the mean. The survey data were then transferred to ASCII files that were edited using LOTUS123. The LOTUS editing consisted of the deletion of unnecessary data and the formatting of the data into files that could be read by a FORTRAN code. These files were then assembled into two large data files and formatted by the FORTRAN program into spatial coordinate and velocity information files which were to be read into PLOT3D. The data from these files were then plotted using PLOT3D on a Silicon Graphics Indigo workstation [Ref. 13].

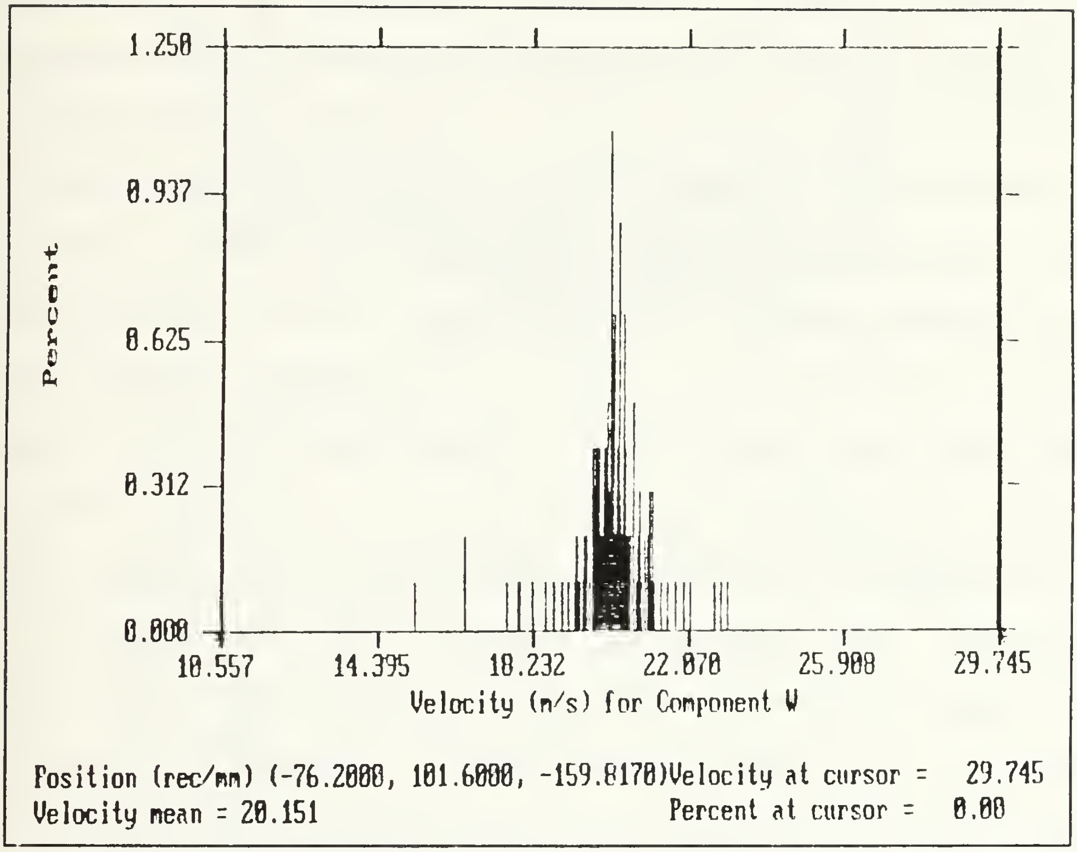

Figure 13. Histogram from FIND 3.5 Statistical Program

IV. RESULTS AND DISCUSSION

A. UPSTREAM PNEUMATIC RAKE PROBE DATA

The inlet flow was nearly uniform near mid-span as shown by Figures 14 and 15. Port 12 (Figure 14) on the pneumatic rake probe is the total pressure port closest to the center of the rake at one inch off center. The slight nonuniformity in the coefficient of pressure, C_p, is due to the wakes from the inlet guide vanes not being fully mixed out prior to reaching the upstream traverse slot. The five inch pitchwise traverse location covers the inlet flow to the passage between blades seven and eight where all the LDV data were acquired. Figure 15 shows the spanwise C_p distribution at a position that was in the middle of the blade passage upstream of blades seven and eight. The approaching boundary layer was about 2.5 or 3.0 inches thick at this position which was nine inches upstream of the blade leading edge. Figures 16 through 21 depict the non-uniformity of the C_p distribution within the turbulent boundary layer itself. All the tabulated C_p values are presented in Apperdix C.

B. DOWNSTREAM PNEUMATIC RAKE PROBE DATA

Downstream pneumatic rake probe data were used to check for flow periodicity and to approximate the location of the vortices. Figure 22 shows the periodicity of the downstream

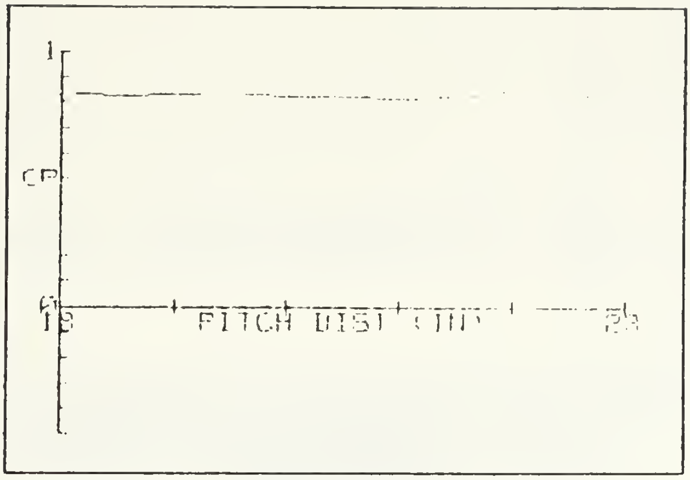

Figure 14. Upstream Pitchwise Pressure Distribution 6.0 Inches from the North Wall

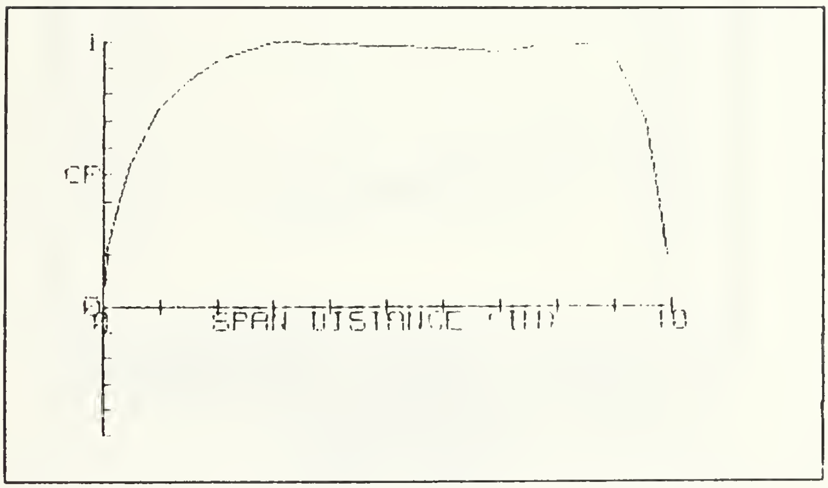

Figure 15. Upstream Spanwise Pressure Distribution for Station 6

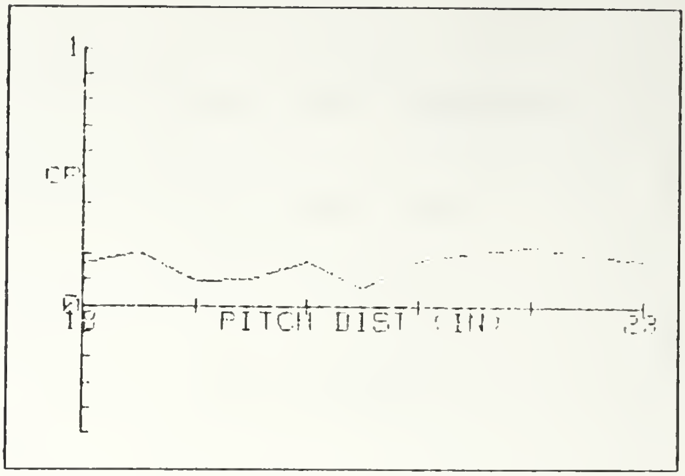

Figure 16. Upstream Pitchwise Pressure Distribution 0.03125 Inches from the North Wall

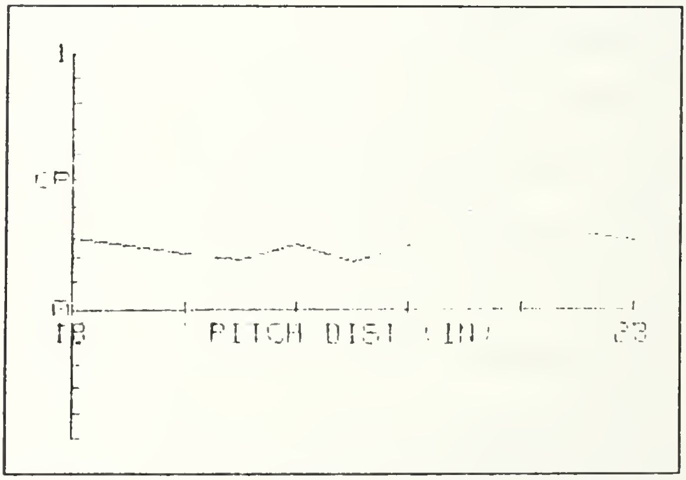

Figure 17. Upstream Pitchwise Pressure Distribution 0.09375 Inches from the North Wall

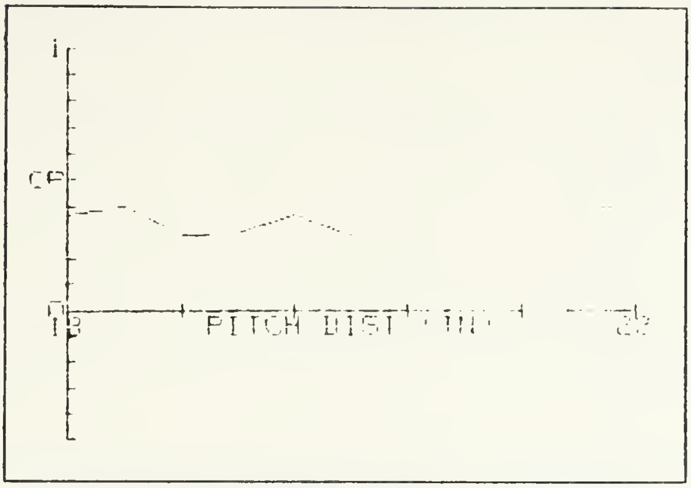

Figure 18. Upstream Pitchwise Pressure Distribution 0.21875 Inches from the North Wall

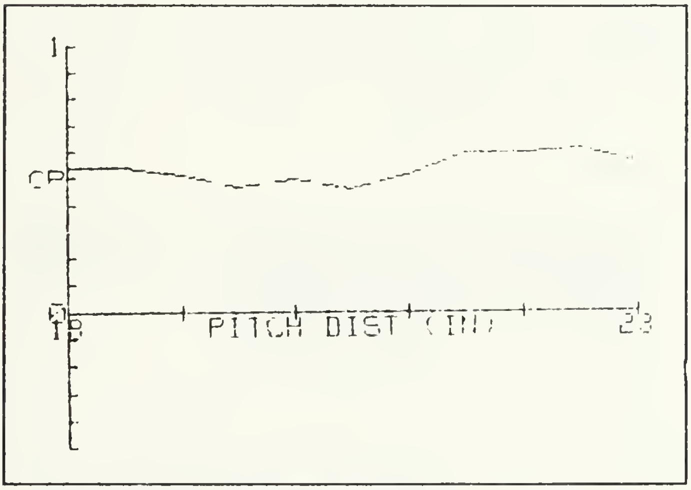

Figure 19. Upstream Pitchwise Pressure Distribution 0.46875 Inches from the North Wall

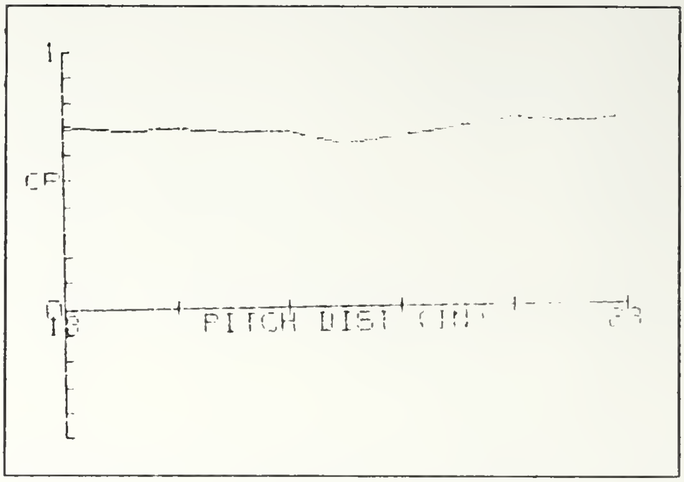

Figure 20. Upstream Pitchwise Pressure Distribution 0.96875 Inches from the North Wall

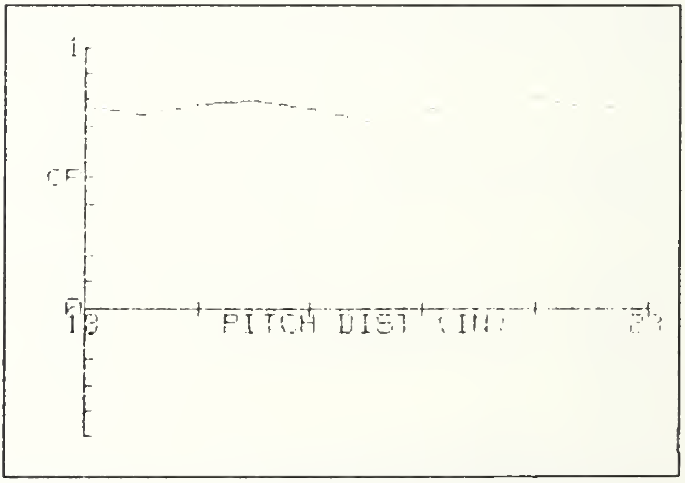

Figure 21. Upstream Pitchwise Pressure Distribution 1.46875 Inches from the North Wall

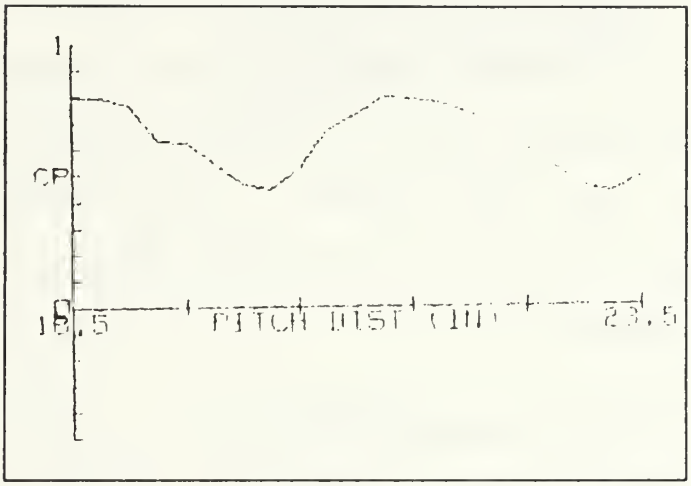

Figure 22. Downstream Pitchwise Pressure Distribution 6.0 Inches from the North Wall

flow. The data are taken again from port 12. Blade trailing edges are located at 19.5 and 22.5 inches in this plot. Figures 21, 23 and 24 show the pitchwise C_p distributions for ports six, seven and eight. Their respective positions on the rake were at 1.46875, 2.0 and 3.0 inches from the wall. The minimums in C_p are points that are within wakes, which contain the vortex system. The C_p minimums show the distortion of the wake since the pitchwise location of each minimum changes with every total pressure port on the rake probe. The outlet tailboards of the cascade were set at four degrees deviation angle and the distance from the blade trailing edges to the traverse slot was nine inches. The measured mid-span deviation angle from the blade trailing edges at the traverse slot was 3.2 degrees.

C. UPSTREAM LDV DATA WITH RE_C=240000

Upstream LDV data were acquired at station 1 at the same x coordinate intervals as the pneumatic rake probe surveys. Figures 25 through 27 show that the flow one inch from the center of the test section is almost strictly two-dimensional. Any deviation from two dimensionality during this survey may be attributable to vorticity production from the inlet guide vanes or the seeding wand. The seeding wand was cylindrical, and in a uniform flow it would shed vortices. Figures 28 through 33 show a nonuniform velocity distribution that increases in nonuniformity as the distance to the test

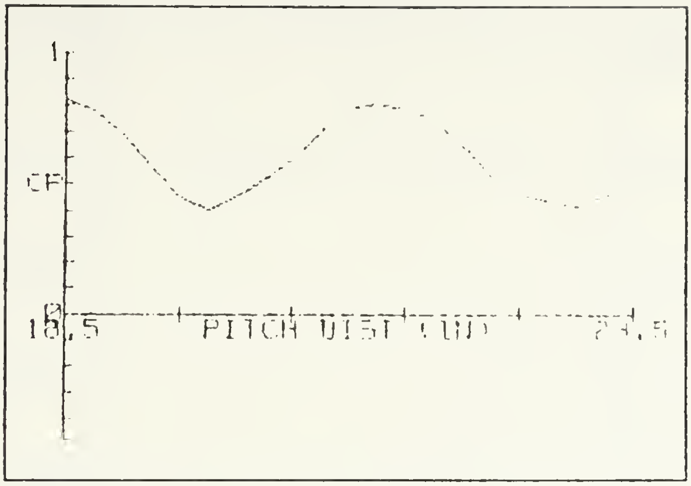

Figure 23. Downstream Pitchwise Pressure Distribution 2.0 Inches from the North Wall

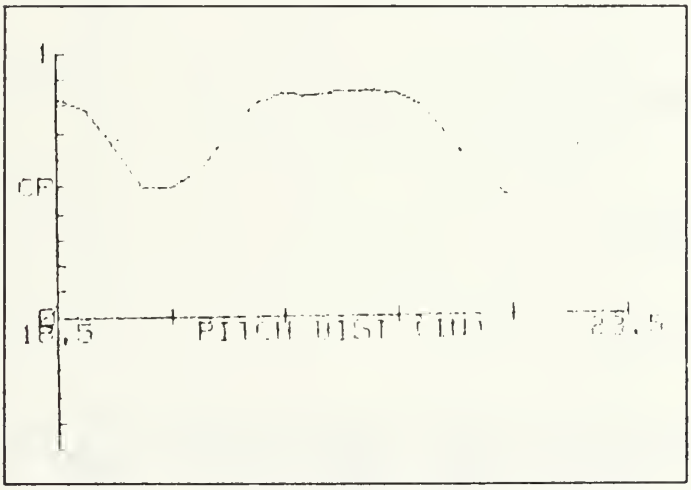

Figure 24. Downstream Pitchwise Pressure Distribution 3.0 Inches from the North Wall

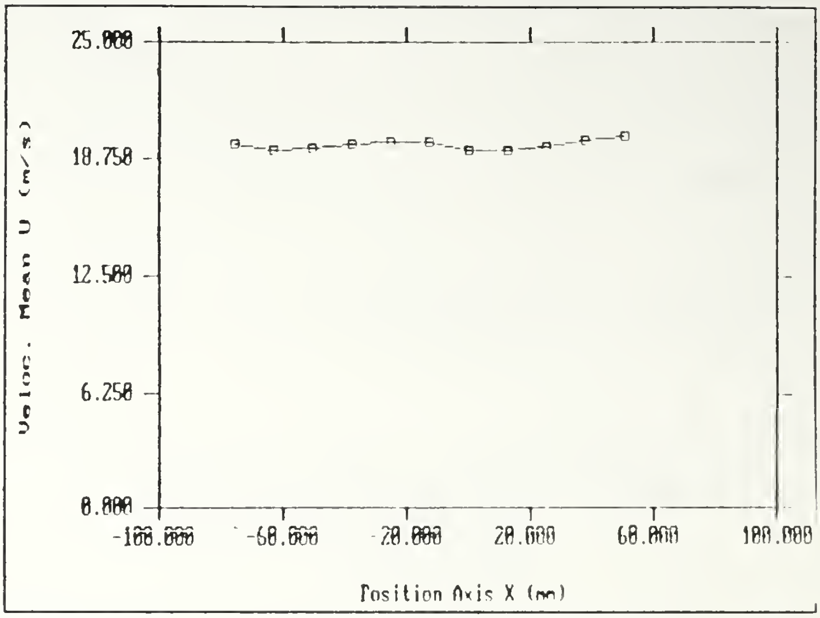

Figure 25. Inlet Pitchwise Survey of the Pitchwise Velocity 4.0 Inches from the Endwall at Station 1

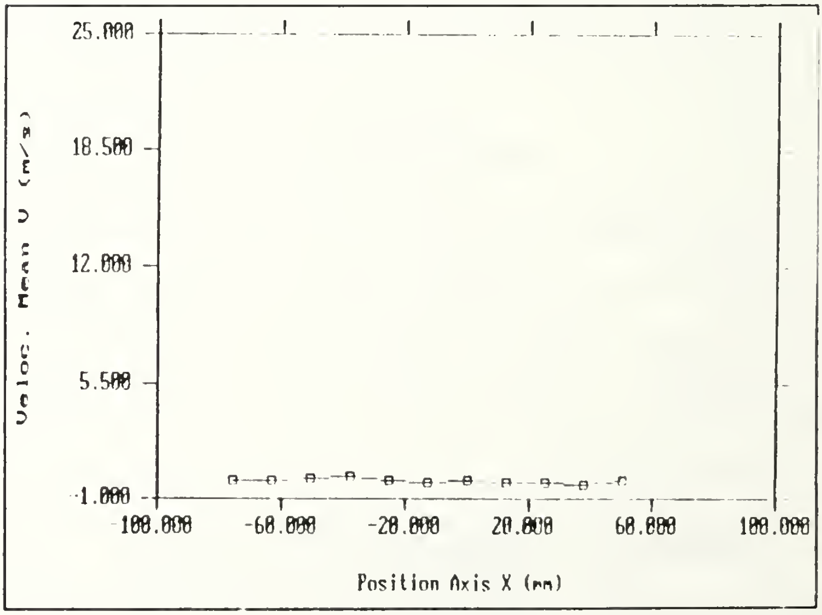

Figure 26. Inlet Pitchwise Survey of the Spanwise Velocity 4.0 Inches from the Endwall at Station 1

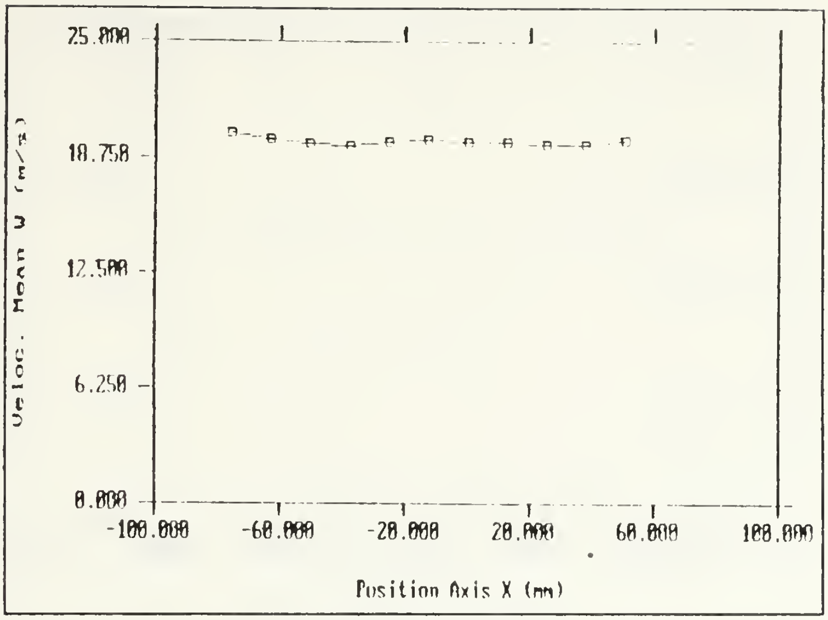

Figure 27. Inlet Pitchwise Survey of the Axial Velocity 4.0 Inches from the Endwall at Station 1

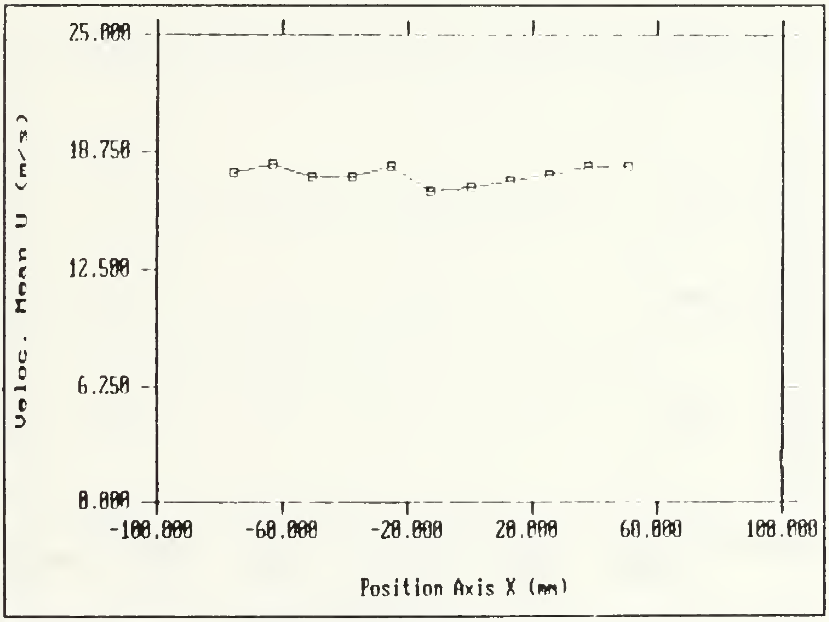

Figure 28. Inlet Pitchwise Survey of the Pitchwise Velocity 0.75 Inches from the Endwall at Station 1

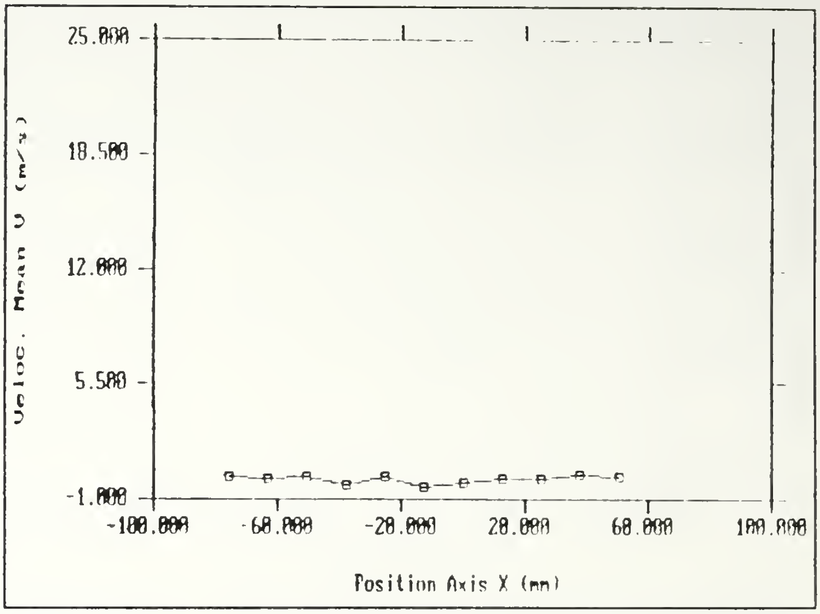

Figure 29. Inlet Pitchwise Survey of the Spanwise Velocity 0.75 Inches from the Endwall at Station 1

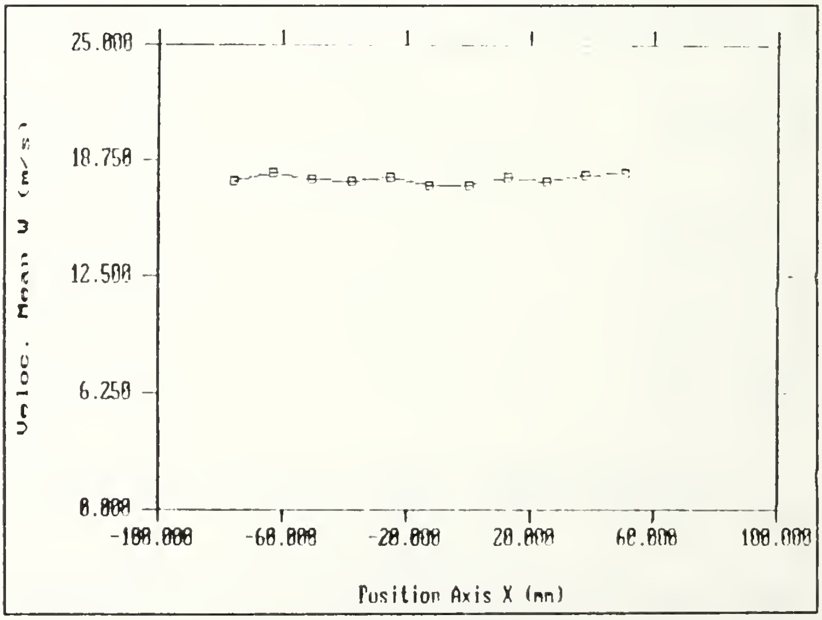

Figure 30. Inlet Pitchwise Survey of the Axial Velocity 0.75 Inches from the Endwall at Station 1

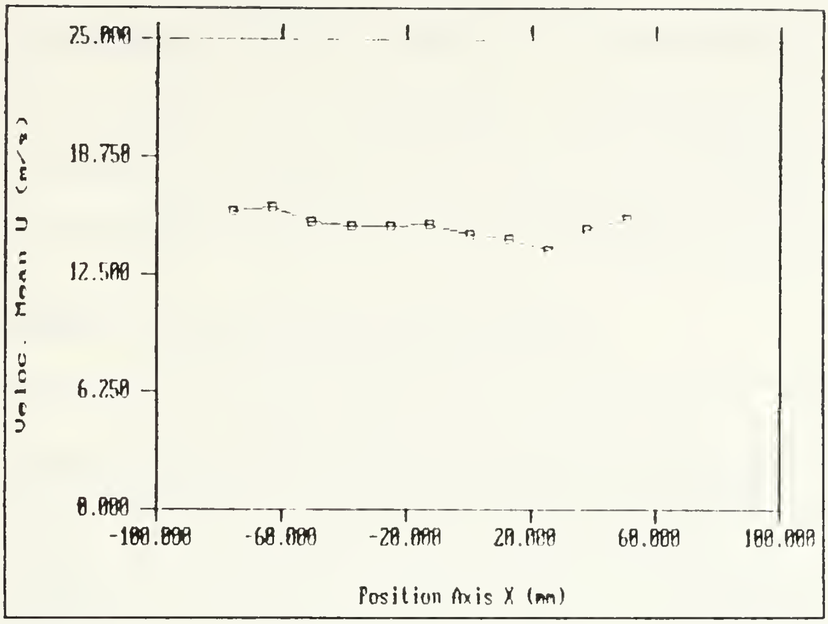

Figure 31. Inlet Pitchwise Survey of the Pitchwise Velocity 0.25 Inches from the Endwall at Station 1

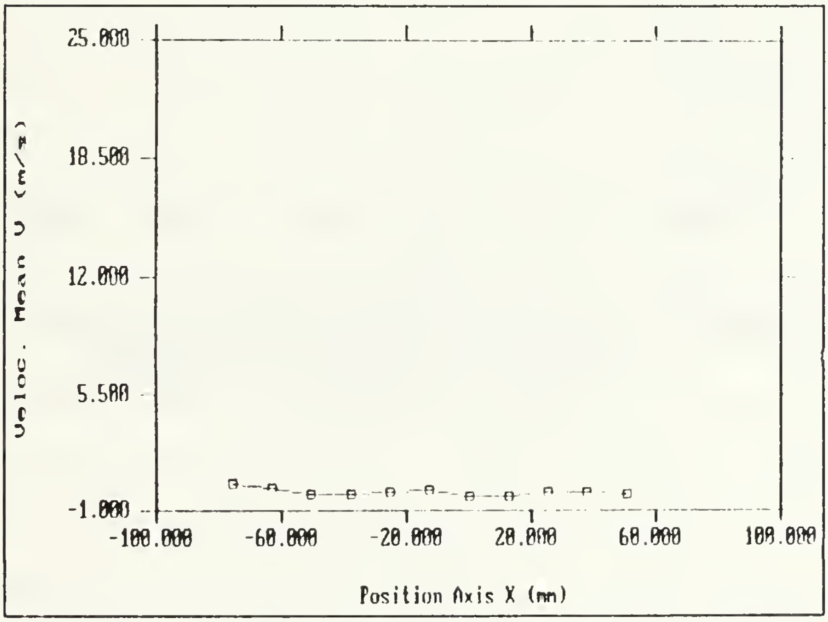

Figure 32. Inlet Pitchwise Survey of the Spanwise Velocity 0.25 Inches from the Endwall at Station 1

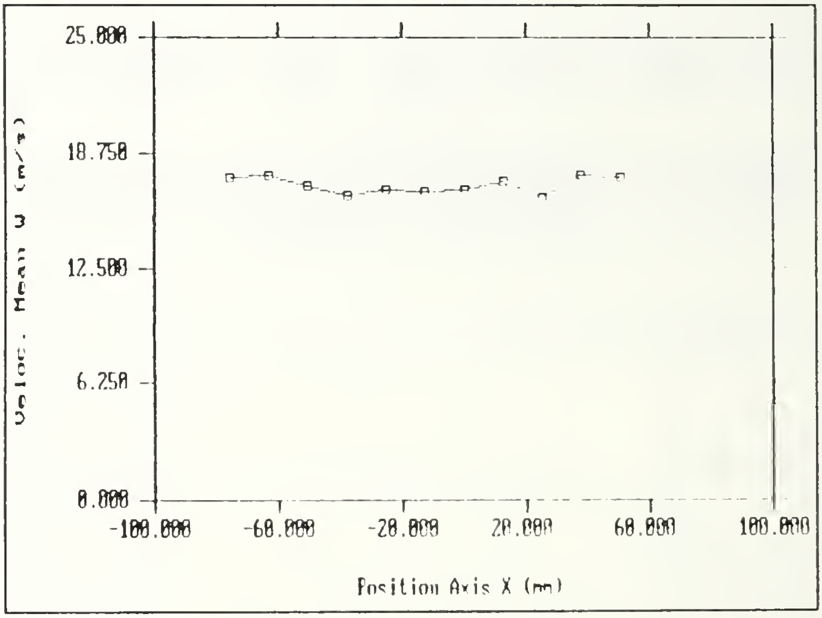

Figure 33. Inlet Pitchwise Survey of the Axial Velocity 0.25 Inches from the Endwall at Station 1

section window decreases. These two surveys were conducted within the turbulent boundary layer. As the distance from the test section window was decreased, keeping the pitchwise dimension constant, the magnitude of the total velocity vector decreased, as would be expected in a turbulent boundary layer.

D. DOWNSTREAM LDV DATA WITH RE_C=240000

Downstream LDV surveys were conducted at station 19. The length of the surveys extended one inch either side of a blade passage. This allowed a check of flow periodicity. A total of eight spanwise LDV surveys were conducted downstream for a finer data grid. The expected results were the velocity characteristics of a clockwise rotating vortex as viewed from the top of the test section. The primary characteristics for identification of the vortex boundaries were spanwise changes in the sign of the u velocity component and pitchwise changes in the sign of the v velocity component. Figures 34 and 35 show a significant change in sign of the u velocity component as the distance from the test section window was decreased from 0.75 inches to 0.50 inches. Figure 36 shows that the v velocity component changed sign from positive to negative and back to positive from the pressure side of one blade to the suction side of the next. Figure 37 is a sketch of the overall secondary flow that exists within a blade passage.

Figure 38 is a velocity field plot of the u and v velocity components in the x-y plane. The pattern shown in the plot is

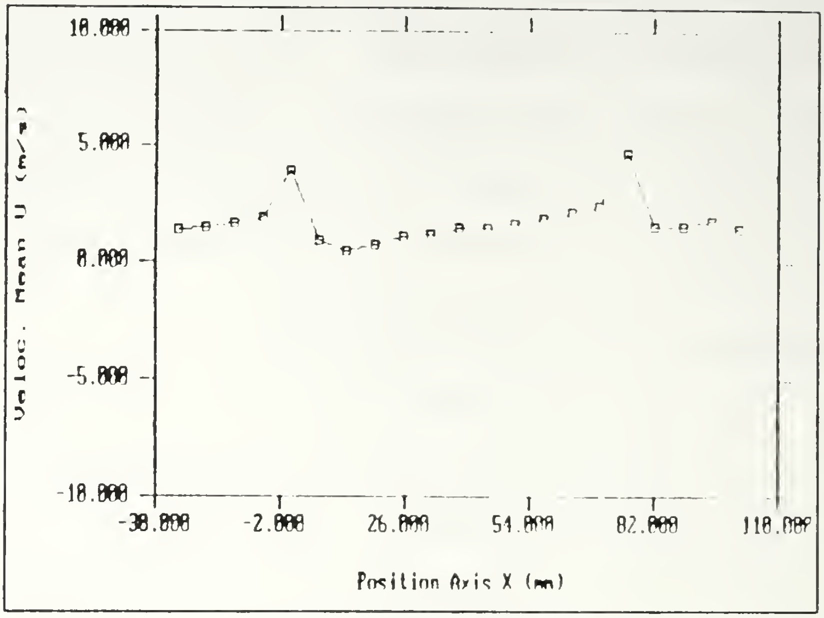

Figure 34. Downstream Pitchwise Survey of the Pitchwise Velocity 0.75 Inches from the Endwall at Station 19

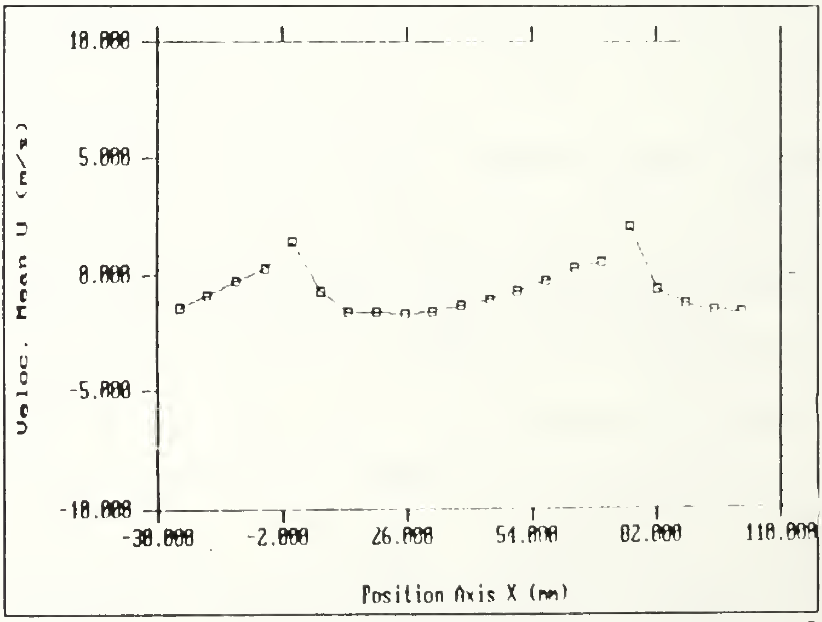

Figure 35. Downstream Pitchwise Survey of the Pitchwise Velocity 0.5 Inches from the Endwall at Station 19

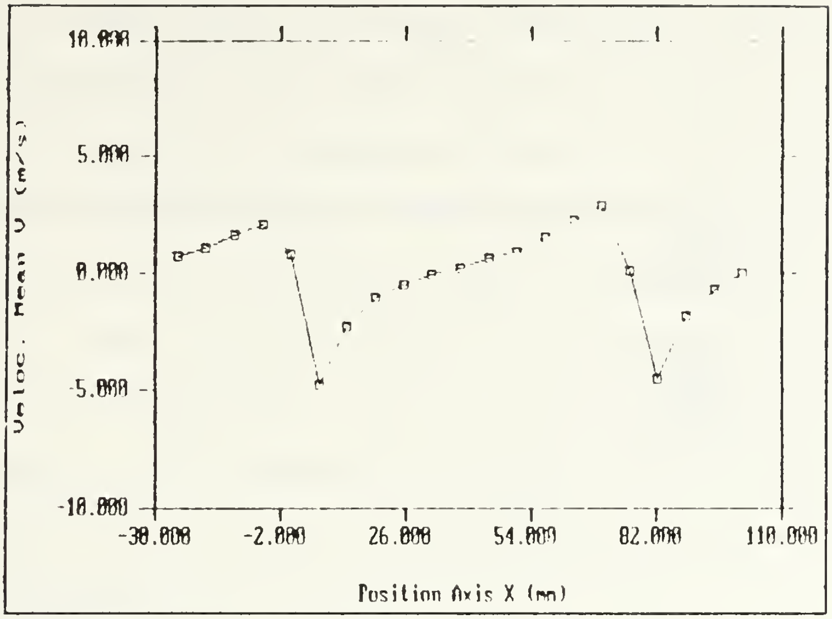

Figure 36. Downstream Pitchwise Survey of the Spanwise Velocity 0.75 Inches from the Endwall at Station 19

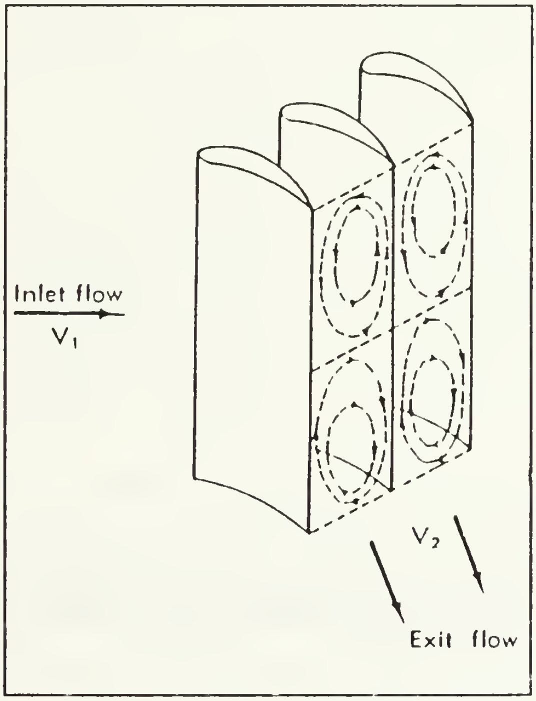

Figure 37. Secondary Flow Due to Case Wall Boundary Layers

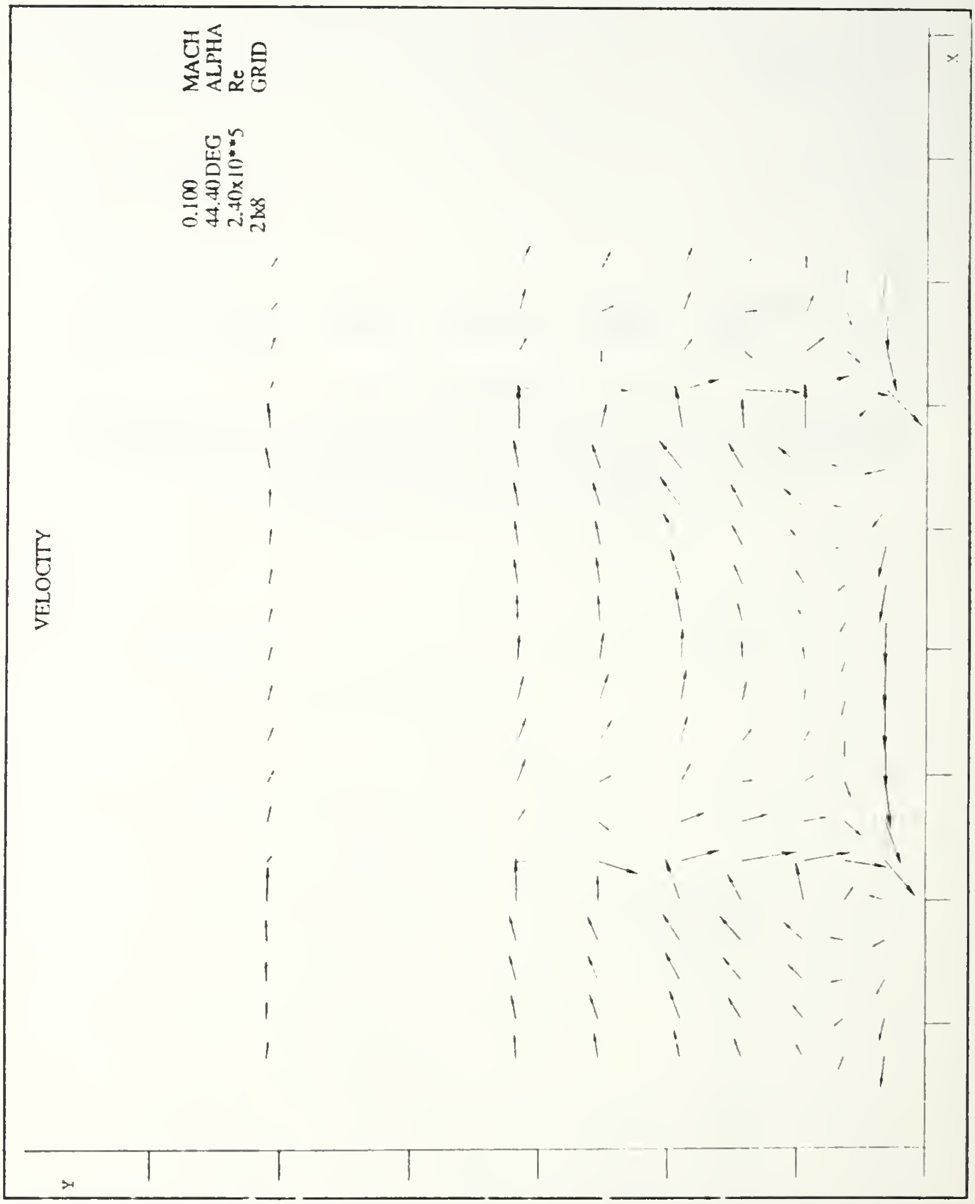

Figure 38. Velocity Field in the Exit Plane at Station 19

the result of the vortex flow from the endwall boundary layer - blade interaction, and the overall secondary flow. The scale for this plot is x ranging from -40 mm to 140 mm and y ranging from 0 mm to 120 mm. Blade trailing edges are located at x=0 mm and x=76.2 mm and the test section window is along the x axis. The velocity vectors are scaled by a factor of 1.5 times their magnitude. The maximum velocity in the plot is 5.16 m/sec. The clockwise rotating vortices are evident and the plot also shows the periodicity of the clockwise rotating vortex.

Figure 39 is a plot of the z component of vorticity [Ref. 13]. The scale for this plot is x ranging from -40 mm to 160 mm and y ranging from 0 mm to 140 mm. The clockwise rotating vortices have been pushed out over the blade trailing edges and remain close to the test section window. A vortex located in a transverse flow will experience lift. This is the situation that is evident in Figure 39, which shows the result of the interaction between the overall secondary flow (Figure 37) with the vortex flow (Figure 1). The clockwise rotating vortex will experience a lift force toward the test section window and hence remain close to the endwall. The counterclockwise rotating vortex forms along the suction side of the blade. The overall secondary flow parallel to the test section window interacts with this counterclockwise rotating vortex and produces a lift force that moves the vortex away from the endwall surface along the blade. The overall

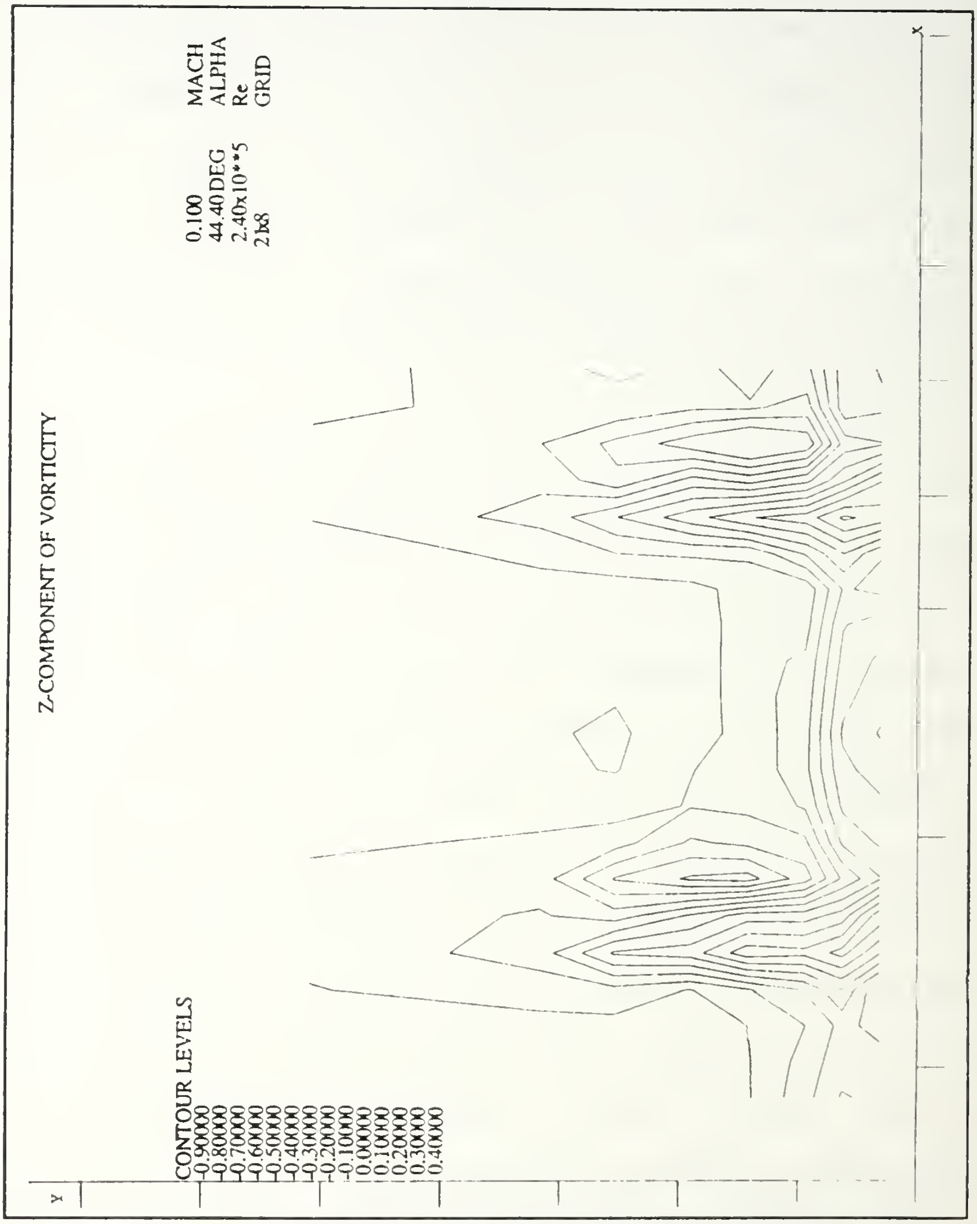

Figure 39. Z-Component of Vorticity in the Exit Plane at Station 19

secondary flow then turns along the blade toward mid-span (Figure 37). The interaction of the overall secondary flow with the counterclockwise rotating vortex, which has been displaced along the blade, now produces a lift force that displaces the vortex into the blade passage. The counterclockwise rotating vortex has therefore been pushed away from the window and into the blade passage.

E. DOWNSTREAM LDV DATA WITH RE_C=711000

Downstream LDV surveys were conducted at station 19 at a Reynolds number of 711000. The length of the pitchwise surveys allowed mapping of the flow field across one blade space. Figures 40 through 45 display the results for the four pitchwise surveys closest to the test section window. Due to the increased inlet flow velocity the vortex system downstream was expected to be much smaller in size. The same criteria for identifying the vortex boundaries were used for this data set. The u velocity component changes sign between 0.60 and 0.40 inches from the test section window as shown in Figure 40. Figure 42 shows a sign change in the v velocity component.

Figures 41, 43 and 45 are standard deviation plots which indicate turbulence intensity. FIND 3.5 will plot measured turbulence intensities but they are referenced to the magnitude of the local velocity component. This makes for extremely high turbulence intensity percentages for the u and

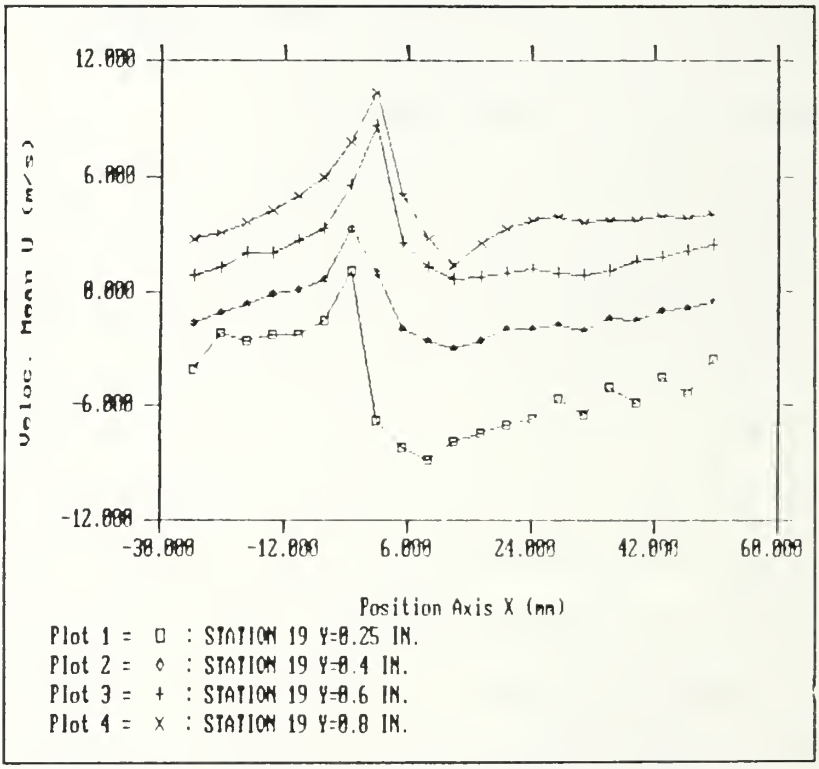

Figure 40. Downstream Pitchwise Surveys of the Pitchwise Velocity at Various Distances from the Endwall at Station 19

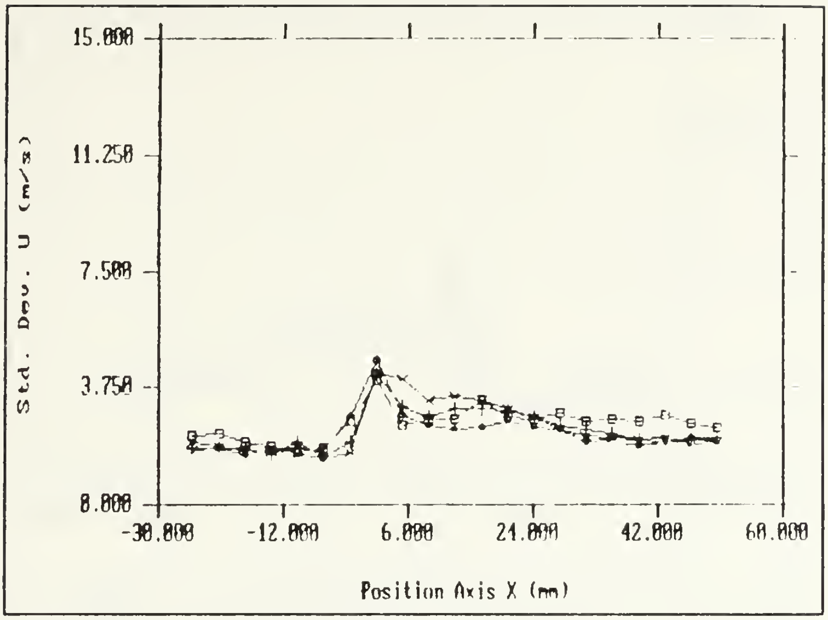

Figure 41. Standard Deviation of the Pitchwise Velocity at Various Distances from the Endwall at Station 19

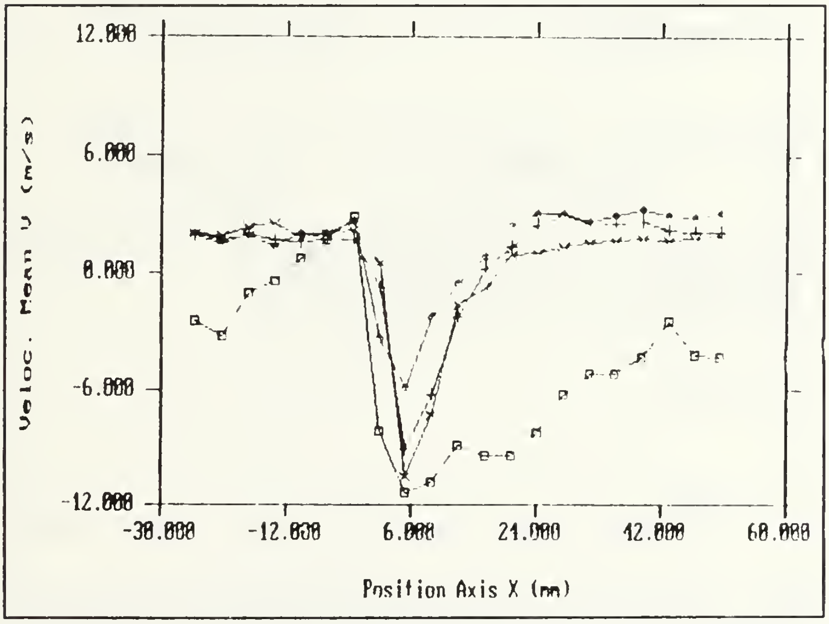

Figure 42. Downstream Pitchwise Surveys of the Spanwise Velocity at Various Distances from the Endwall at Station 19

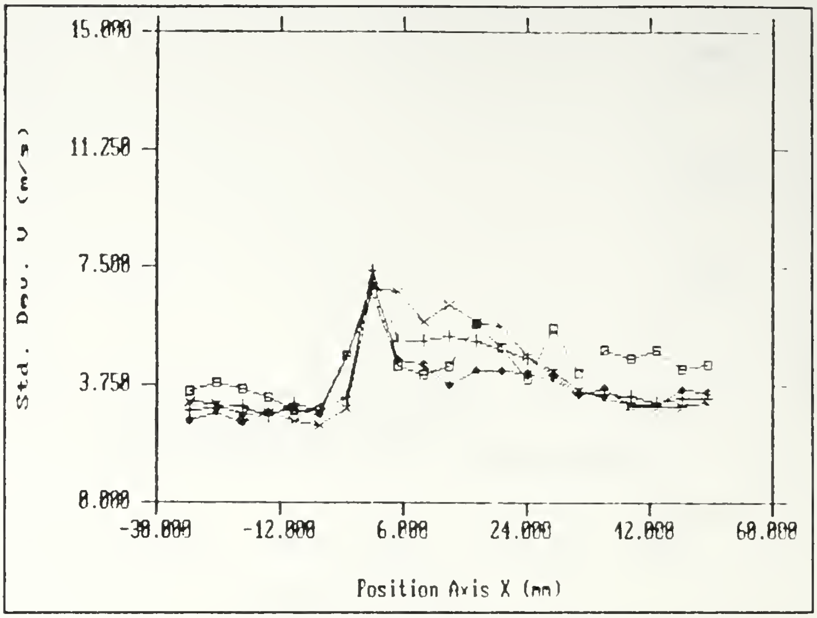

Figure 43. Standard Deviation of the Spanwise Velocity at Various Distances from the Endwall at Station 19

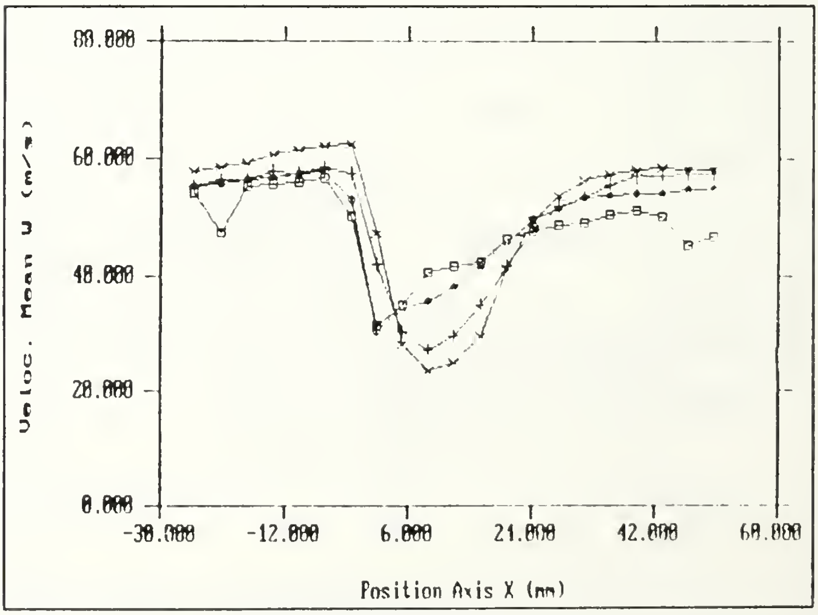

Figure 44. Downstream Pitchwise Surveys of the Axial Velocity at Various Distances from the Endwall at Station 19

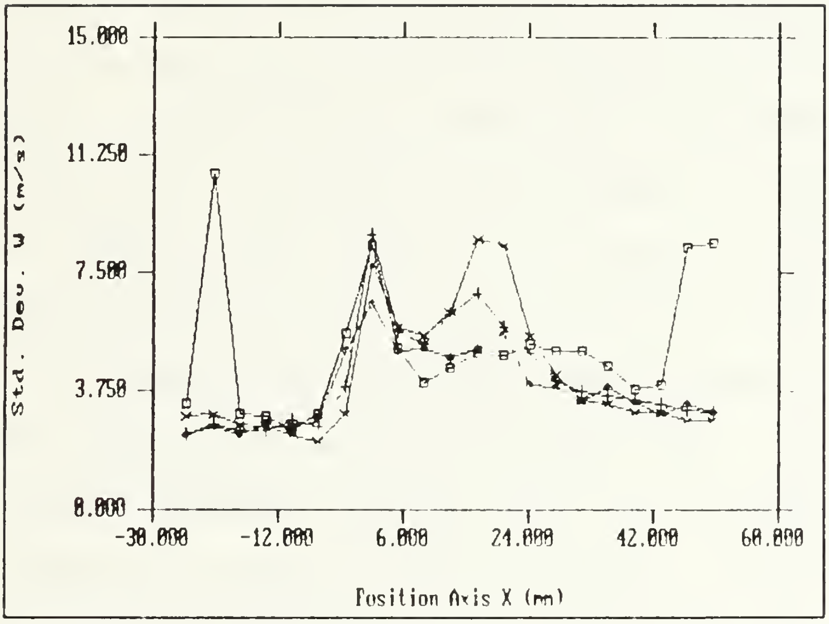

Figure 45. Standard Deviation of the Axial Velocity at Various Distances from the Endwall at Station 19

v velocity components. A better measure for turbulence intensity would be to reference them to the total magnitude of the inlet velocity.

Figure 46 is a plot of the downstream velocity field in the x-y plane. The x axis scale ranges from -40 mm to 60 mm with the test section window lying along the x axis. The y axis scale ranges from 0 mm to 70 mm. Velocity vectors are scaled by a factor of 0.5 in this plot. The maximum velocity magnitude in this velocity field in 11.4 m/sec. The clockwise rotating vortex is very evident in this figure. Figure 47 is a plot of the z component of vorticity. This plot has the same scaling as Figure 46. A blade trailing edge is located at 0 mm. The clockwise rotating vortex has been pushed closer to the test section window by the secondary flow when compared to Figure 39. The size of the vortex is also much smaller as can be expected at this higher Reynolds number. The counterclockwise rotating vortex is about the same distance away from the window but it is slightly closer to the blade surface when compared to Figure 39. The plot also shows that the counterclockwise rotating vortex has been significantly distorted into two counterclockwise rotating cells. There are also some weak secondary vortices further out in the blade passage away from the window. Figure 48 is a plot of the axial velocity component at station 19 for other pitchwise surveys further away from the endwall. If a comparison is made of the maximum deficit points in the wake for Y=0.4

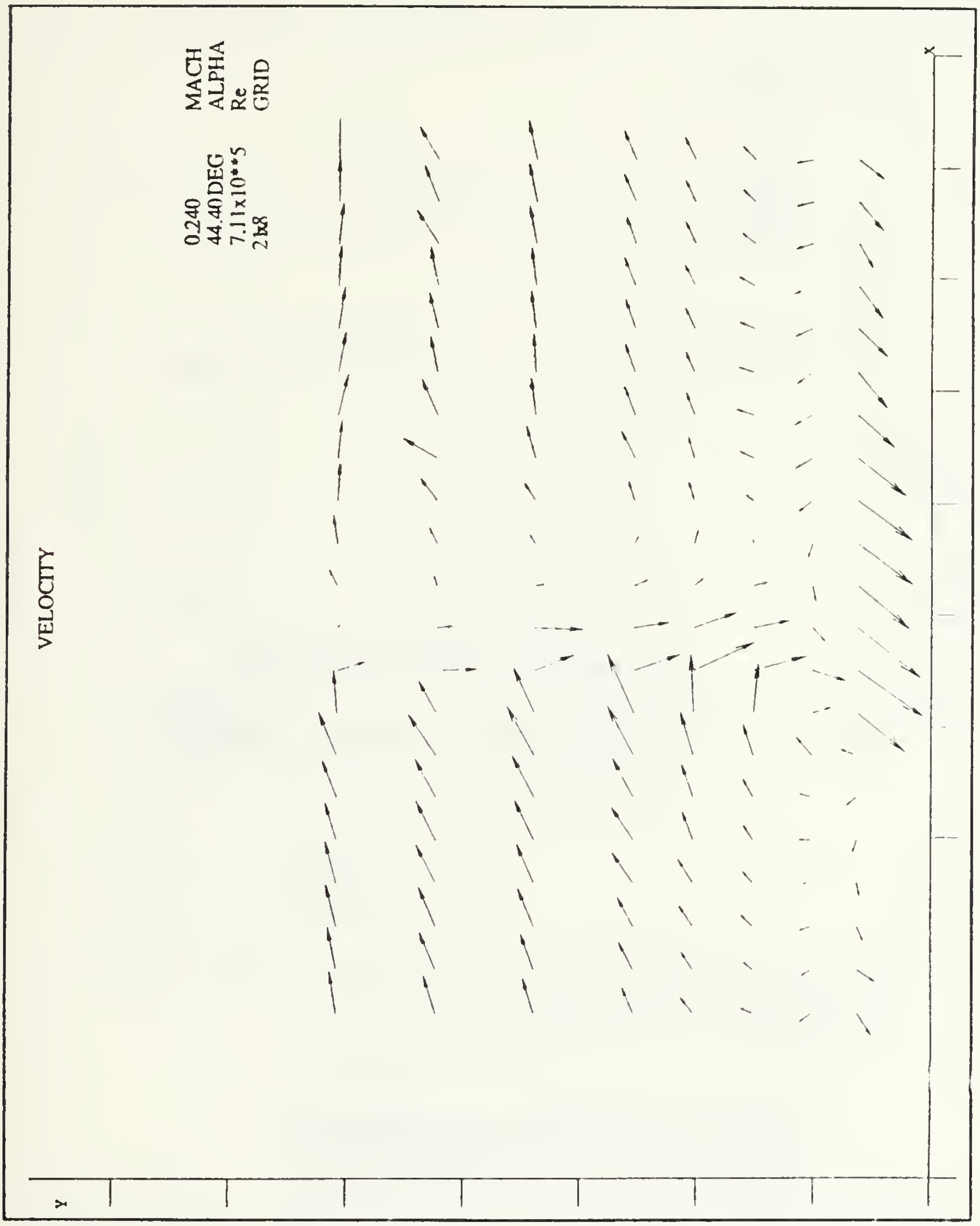

Figure 46. Velocity Field in the Exit Plane at Station 19

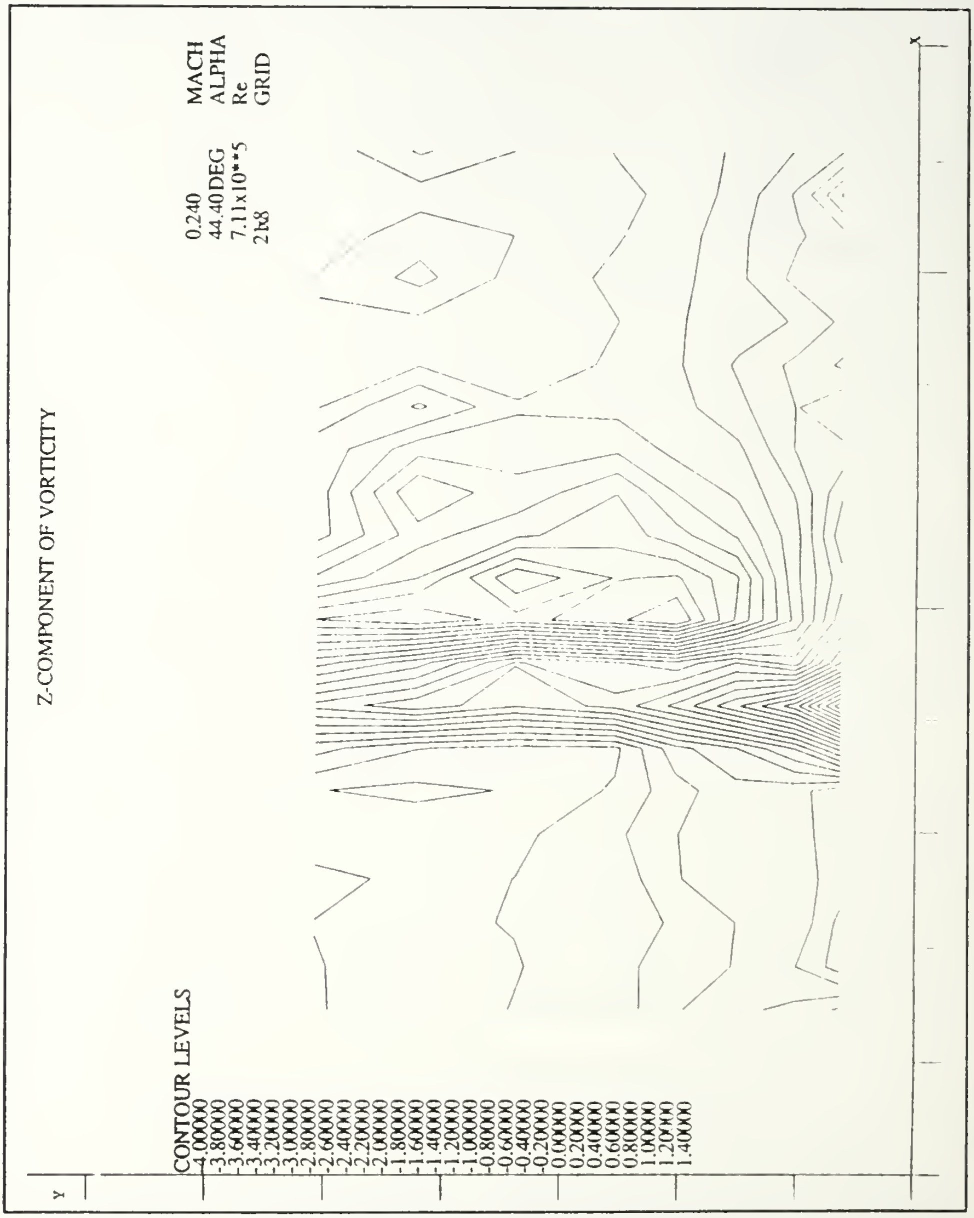

Figure 47. Z-Component of Vorticity in the Exit Plane at Station 19

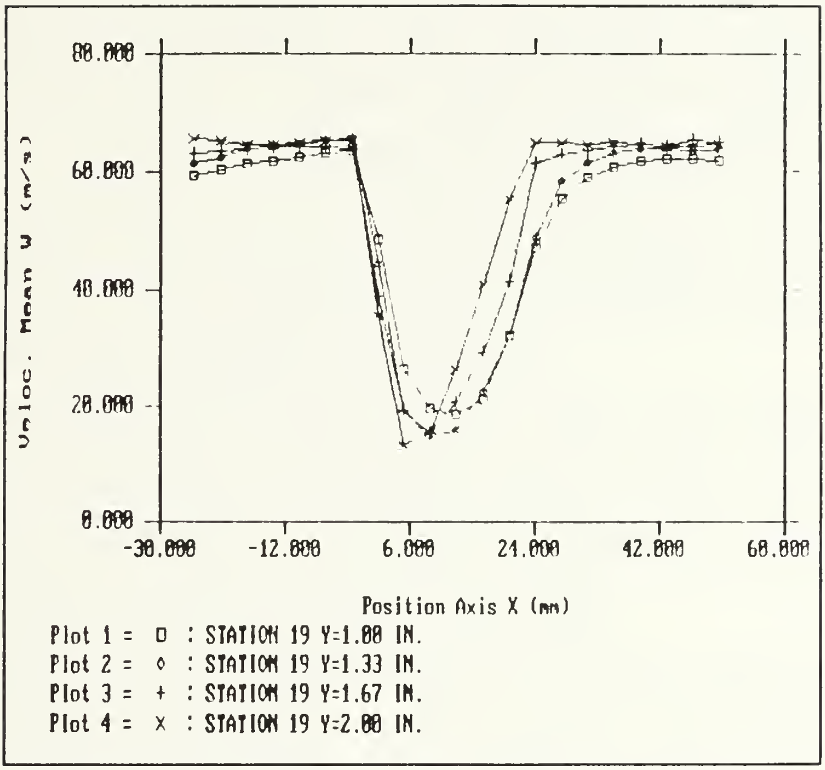

Figure 48. Downstream Pitchwise Surveys of the Axial Velocity at Various Distances from the Endwall at Station 19

inches and Y=0.6 inches from Figure 44 and Y=2.00 inches from Figure 48 the maximum deficit points will not form a straightline. This is most probably as a result of the two counter-rotating vortices interacting with each other.

V. CONCLUSIONS AND RECOMMENDATIONS

A three-component LDV system with traverse was successfully set-up and used to obtain measurements of three-dimensional viscous effects in a compressor cascade. The validation of fully three-dimensional CFD analysis of cascade flows should eventually lead improved methods for turbomachinery design. Current axial machine design methods are based on largely two-dimensional empirical data, such as given in NASA SP-36 [Ref. 14]. Three-dimensional viscous flow analysis should lead to better loss predictions and therefore to more efficient turbomachine designs.

The upstream LDV surveys showed the inlet flow to be nearly two-dimensional. The slight nonuniformity of the inlet flow may be attributable to vorticity production from either the inlet guide vanes or the seeding wand.

The results of the downstream LDV surveys nearly matched pre-experiment expectations. The counter rotating vortices were produced by the endwall boundary layer and blade tip interaction. The downstream vortices must be approximately the same strength. If one vortex was dominant it would consume the other since they are counter rotating. The effect of the overall secondary flow within the blade passage was more than expected. The overall secondary flow effect was extremely evident in the higher Reynolds number flow since the

clockwise rotating vortex was displaced over the blade trailing edge next to the test section window. The appearance of several weak vortices in the blade passage away from the test section window during the higher Reynolds number surveys is unexplained. If the sources of these vortices are the inlet guide vanes then any conclusions drawn from the flow within this cascade are facility specific. This would hold true for this cascade and any other cascade that utilizes inlet guide vanes to turn the upstream flow to a particular flow angle.

Several recommendations are made for LDV equipment procurement. The LDV system should be operated with a collimator installed between the laser source and the Colorburst. This will reduce the beam diameter of the incoming laser beam and will result in increased power in the fringes. The procurement and utilization of a set of probe beam expanders is recommended. This would increase the power in the fringes by an order of magnitude and consequently increase the system's signal to noise ratio. Acquisition of an IFA 750 digital burst correlator would decrease the time required to obtain data and would simplify the data acquisition process, but is not required.

Follow-up three-component LDV analysis of the weak vortices that exist in the blade passage must be completed. A finer grid of data points must be acquired and analyzed in this region under the same tunnel conditions to verify the

existence of these weak vortices. Subsequent upstream surveys would need to be conducted to determine if the inlet guide vanes are the sources of these vortices. Additional downstream surveys need to be done at different axial stations to map the migration of the endwall vortices downstream of the trailing edges. The secondary flow in the blade passage also needs to be mapped and attempts should be made to measure the hypothesized three-dimensional reattachment of the leading edge separation bubble [Ref. 15].

Further LDV data acquisition could be conducted at various Reynolds numbers with the cascade in its current configuration in an attempt to quantify any Reynolds number effects on the flow characteristics.

APPENDIX A. PNEUMATIC RAKE PROBE SOFTWARE

A. INTRODUCTION

Total and static pressure data were acquired using a 20 hole rake probe upstream and downstream of the controlled-diffusion blades. This 20 hole pneumatic rake probe covered the entire ten inch span of the test section. The probe design and calibration are described by Webber [Ref. 8]. Information on boundary layer profiles, total pressure gradients, and static pressure gradients was desired. The pressure data were acquired and processed by a program named ACQUIRE4. The program was written in HP BASIC and was a modification of ACQUIRE that was written by Classick [Ref. 9]. The major modifications included: Scanivalve port assignments for the 20 hole pneumatic rake probe, utilization of one Scanivalve for measurements, scanning only the Scanivalve ports of interest for this work, and processing the data from the Scanivalve ports of interest both numerically and graphically. Webber completed further program modifications in February 1993 to include: rake probe total pressure printouts, addition of a test section Prandtl probe, acquisition of plenum pressure and temperature data, addition of a calibration polynomial to compute the flow angle the rake probe was sensing, and axial velocity computation. ACQUIRE4

utilizes a subprogram named SUBACQUIRE2 for Scanivalve positioning and reading the digital voltmeter. SUBACQUIRE2 is unchanged as written by Classick [Ref. 9].

1. Program Execution

This section will outline the steps required to run ACQUIRE4. It will also outline the ramifications of selecting certain options available to the user during the execution of ACQUIRE4. The steps listed here in the program execution subsection need to be followed in the order that they are listed.

1. Equipment turn on and computer boot up procedures remain the same as outlined by Classick [Ref. 9].

2. Press f5 corresponding to the soft key label LOAD. See Figure A1 for keyboard and soft key labels.

3. Type /CLASSICK/PROGS/ACQUIRE4 between the quotation marks and press RETURN. This establishes the path from the root directory where the CLASSICK directory is located to file ACQUIRE4 via the subdirectory PROGS.

4. Press f3 corresponding to the soft key label RUN. The first prompt in the ACQUIRE4 program will appear. The prompt will read,"NAME THE FILE FOR THE RAW DATA TO BE COLLECTED FROM THE PROBE(S)". Utilize either letters or numbers or both to name the raw data file. Use up to ten characters for the file name. Do not use spaces or quotation marks. After naming the file press RETURN.

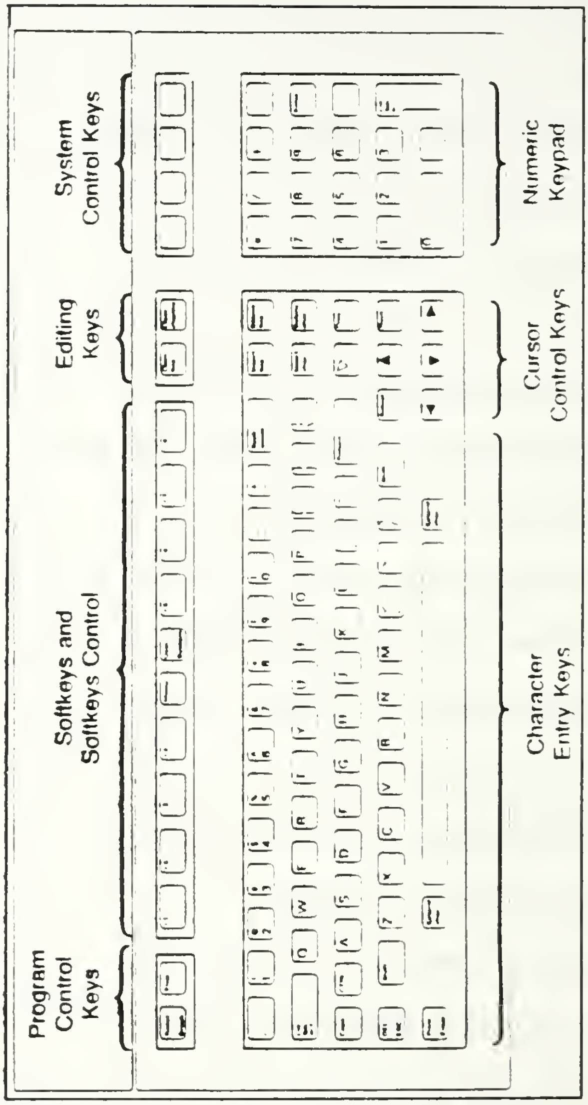

Figure A1. Keyboard Diagram

5. At the next prompt type in the scaled data file name and press RETURN.

6. The program will now ask for the rake probe angle from the horizontal. Enter the rake probe angle in degrees and press ENTER.

7. The next prompt will ask for the atmospheric pressure in inches of mercury. Type in the pressure, e.g., 29.92. Press RETURN. Atmospheric pressure should remain fairly constant throughout the duration of the rake probe survey. In the unlikely event of a significant atmospheric pressure change during a rake probe survey the atmospheric pressure can be changed during program execution. To the change the atmospheric pressure perform the following steps:

a. Press the STOP key next to the f1 key.

b. Type Pbaro 30.00 to change from 29.92 to 30.00.

c. Press RETURN.

d. Press f2 corresponding to the soft key label CONTINUE.

8. The next prompt will ask for scan number and probe position. Scan number is at the discretion of the user. Probe position is the pitch distance along the traverse from the origin in inches. Type in both numbers separated by a comma and press RETURN. Each probe position should be numbered sequentially. This is the station number and it must be recorded by the user. <u>The scan will begin after pressing RETURN</u>. Scanivalve positions 10 through 34 will be scanned.

Positions 15 through 34 are for the rake probe. The other five positions are for a Prandtl probe, atmospheric pressure, calibration pressure, and plenum pressure. Table A1 gives the 25 port assignments. During the scan a table of port, voltage, and gauge pressure will be printed to the screen. Below this table will be the temperature and atmospheric pressure. This should be monitored as data are acquired in order to recognize any obvious erroneous readings. Once the scan is complete the software will normalize the 17 total pressure ports with respect to the highest total pressure reading acquired. A graph of C_p versus span distance will then be plotted on the screen. This plot should also be viewed for any erroneous data.

9. Once this plot is viewed press f2 which corresponds to the soft key label CONTINUE.

10. The next prompt will ask if the data are acceptable. The f1 soft key will now be labeled RECORD and the f4 soft key will be labeled REPEAT. Selection of RECORD will shuffle the rake probe raw and scaled data so the total pressure readings are in consecutive order. Table A2 depicts the new matrix column assignments. RECORD will also store the shuffled data to the files named in steps four and five. Selection of REPEAT will result in a prompt that will ask for the new probe position. Enter the pitch distance from the origin and press RETURN. The scan will be repeated.

TABLE A1. SCANIVALVE PORT ASSIGNMENTS

Scanivalve Port Number	Value Measured
10	Prandtl probe total
11	Prandtl probe static
12	atmospheric pressure
13	calibration pressure
14	plenum total pressure
15	rake probe total
16	rake probe total
17	rake probe total
18	rake probe total
19	rake probe total
20	rake probe total
21	rake probe total
22	rake probe total
23	rake probe static
24	rake probe yaw
25	rake probe yaw
26	rake probe total
27	rake probe total
28	rake probe total
29	rake probe total
30	rake probe total
31	rake probe total
32	rake probe total
33	rake probe total
34	rake probe total

TABLE A2. RAWDAT MATRIX COLUMN ASSIGNMENTS

Rawdat Matrix Column Assignment	Value Stored
10	Prandtl probe total
1[illegible]	Prandtl probe static
12	atmospheric pressure
13	calibration pressure
14	plenum total pressure
15	rake probe total
16	rake probe total
1[illegible]	rake probe total
18	rake probe total
19	rake probe total
2[illegible]	rake probe total
21	rake probe total
22	rake probe total
23	rake probe total
24	rake probe total
2[illegible]	rake probe total
26	rake probe total
27	rake probe total
28	rake probe total
2[illegible]	rake probe total
30	rake probe total
31	rake probe total
32	rake probe static
33	rake probe yaw
34	rake probe yaw

11. The next option will be for the continuation or termination of data collection. The f1 soft key will now be labeled END PRB DATA and the f4 soft key will be labeled GO ON. Selection of END PRB DATA will result in the names of the files which contain the stored raw and scaled data values to be printed to the screen and will lead to the data normalization options. When GO ON is selected the software asks for the new probe position. Enter the new pitch distance and press RETURN. <u>Make certain that the probe is in the new position prior to entering the pitch distance</u>. Steps seven through nine will be repeated for the new probe position.

12. Selection of END PRB DATA leads to a surface plot or print option. Soft key f1 is now labeled SURF and soft key f4 is labeled PRINT. Selection of SURF leads to the surface plot routine. <u>Once SURF is selected the user cannot return to the PRINT option</u>. The SURF option is explained in step 14. Selection of PRINT leads to a prompt for spanwise or pitchwise normalization of the total pressure data.

13. Once PRINT is selected soft key f1 will be labeled SPAN and soft key f4 will be labeled PITCH. Selection of SPAN results in the original scaled data matrix being copied to a different variable name. Each row of the matrix represents one scan of the rake probe at each pitchwise position in the traverse. SPAN will normalize the total pressure data for the rake probe at each pitchwise position with respect to the highest total pressure recorded at each

pitchwise position. The next prompt will ask for which pitchwise station the user would like to print out. Enter the station number and press RETURN. A table of data will be dumped to the printer. After the data table is complete a boundary layer profile plot will appear on the screen. Figure A2 is an example of the spanwise normalization output. Press the f2 soft key to dump this plot to the printer and continue execution of the program. The next prompt will ask if the user would like one of the following options: another spanwise plot, pitchwise normalization, or quit the program. The f1 soft key is now labeled SPAN. The f3 soft key is labeled PITCH. The f4 soft key is labeled QUIT. Selection of SPAN loops back to the prompt asking for the station number to be printed out. Selection of PITCH leads to the pitchwise normalization routine. Selection of QUIT stops program execution. Selection of PITCH from the SPAN/PITCH prompt or the SPAN/PITCH/QUIT prompt once again copies the original scaled data matrix to another variable name. Once PITCH is selected the program cannot go or return to SPAN. During the survey of several pitchwise stations the plenum pressure may fluctuate. The SPAN option assumes a constant plenum pressure for each scan of the probe since each spanwise scan takes less than a minute. Pitchwise normalization must take into account plenum pressure variation since the data is taken over a much longer time interval. For pitchwise normalization the total pressure data for each pitchwise station is normalized with

PRINT OUT FOR STATION 1 , 20 INCHE·

PROBE PORT	CP	[illegible]
1	.2730	.6340
2	.4035	[illegible]
3	.548[illegible]	5.[illegible]
4	.6943	7.[illegible]
5	.8570	[illegible]
6	.9165	[illegible]
7	.9503	10.0100
8	.9580	10.0920
12	.9899	10.4290
13	.9860	10.3860
14	.9905	10.4310
15	1.0000	10.5340
16	.9691	10.2080
17	.7947	8.3690
18	.5974	6.1880
19	.4642	4.8900
20	.3759	3.9600

PRANDTLE TOTAL PRESSURE = 10.604

PRANDTLE STATIC PRESSURE --5.79

PLENUM PRESSURE - 12.095

PLENUM TEMPERATURE = 535.58629

RAKE MEASURED Q = 13.942

FLOW ANGLE (BETA) = 43.324091[illegible] DEG

TOTAL VELOCITY = 272.74939365[illegible] FPS

AXIAL VELOCITY = 198.42090[illegible] FPS

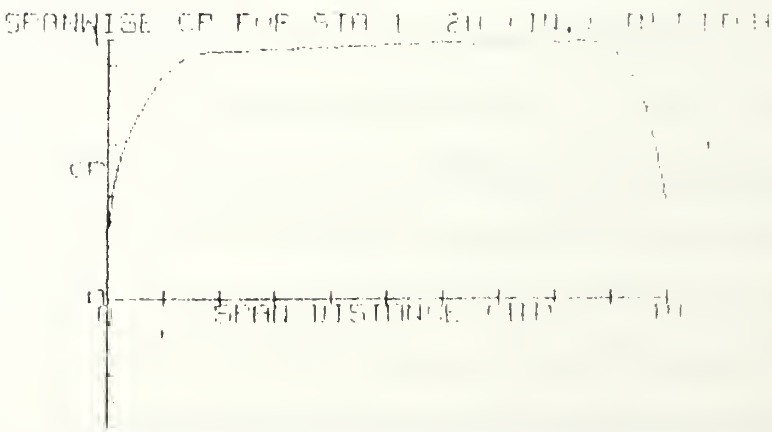

Figure A2. Example of the Output from the Spanwise Normalization Option

respect to the plenum pressure recorded at each corresponding pitchwise station. The program will now prompt the user for which total pressure port the user is requesting data. Enter the port number and press RETURN. A table of pitch distance versus C_p will now be dumped to the printer. After the data table is complete a plot of the same data will appear on the screen. This plot will depict pitchwise total pressure gradients. Figure A3 is an example of the pitchwise normalization output. Press the f2 soft key to dump the plot to the printer and continue execution of the program. The next prompt is for the termination of the pitchwise normalization option or the input of another total pressure port to be analyzed. The f1 soft key will be labeled PITCH and the f4 soft key will be labeled QUIT. Selection of PITCH loops the program back to the total pressure port number input. QUIT leads to another print option.

14. Selection of QUIT from the SPAN/PITCH/QUIT prompt or the PITCH/QUIT prompt leads to an option of printing the pitchwise static pressures. The f1 soft key will be labeled STATIC and the f4 soft key will be labeled QUIT. Selection of STATIC results in a table of static pressure data being dumped to the printer. Figure A4 is an example of the static pressure output. QUIT leads to a surface plot print option.

15. After selecting QUIT from the STATIC/QUIT prompt or after the printing of the static pressure data the program reaches the last prompt. This is the surface plot option.

THIS IS A PRINT OUT FOR PORT 12 LOCATED 5 INCHES
FROM THE NORTH WALL

STATION(IN.)	CP
18.500	.8433
19.000	.8590
19.500	.8440
20.000	.8192
20.500	.8545
21.000	.8329
21.500	.8345
22.000	.8232
22.500	.8467
23.000	.8437
23.500	.8210

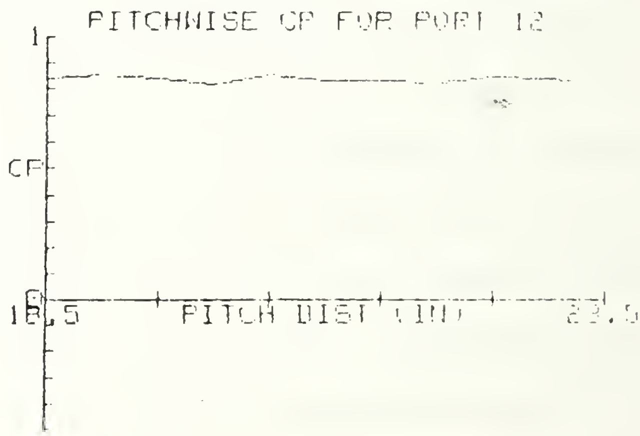

Figure A3. Example of the Output from the Pitchwise Normalization Option

```
*******************************************************************
THIS IS A PITCHWISE PRINT OUT OF PROBE STATIC PRESSURES
      STATION (IN.)                    STATIC PRESSURE
          18.500                            -.3350
          19.000                            -.2540
          19.500                            -.3340
          20.000                            -.3340
          20.500                            -.2940
          21.000                            -.3540
          21.500                            -.3320
          22.000                            -.4300
          22.500                            -.3280
          23.000                            -.3200
          23.500                            -.3180
```

Figure A4. Example of Static Pressure Output

The f1 soft key will be labeled SURF and the f4 soft key will be labeled QUIT. Selecting QUIT stops program execution. Selection of SURF copies the original scaled data matrix to another variable name. Total pressure readings at each station along the traverse are normalized with respect to the plenum pressure reading corresponding to that station. This takes into account plenum pressure variation. The plenum pressure normalized matrix is now searched for the greatest value. All of the plenum pressure normalized values are now normalized by this greatest value. A surface plot now appears on the screen. This surface plot will depict total pressure gradients in either the spanwise or pitchwise directions or both. Figure A5 is an example of the surface plot output. Press the f2 soft key to dump the plot to the printer and terminate program execution.

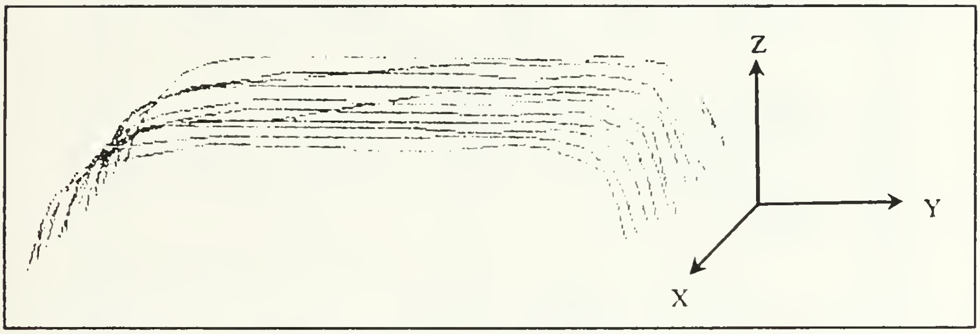

Figure A5. Example of Surface Plot Output

APPENDIX B. LDV DATA FOR RE_C=711000

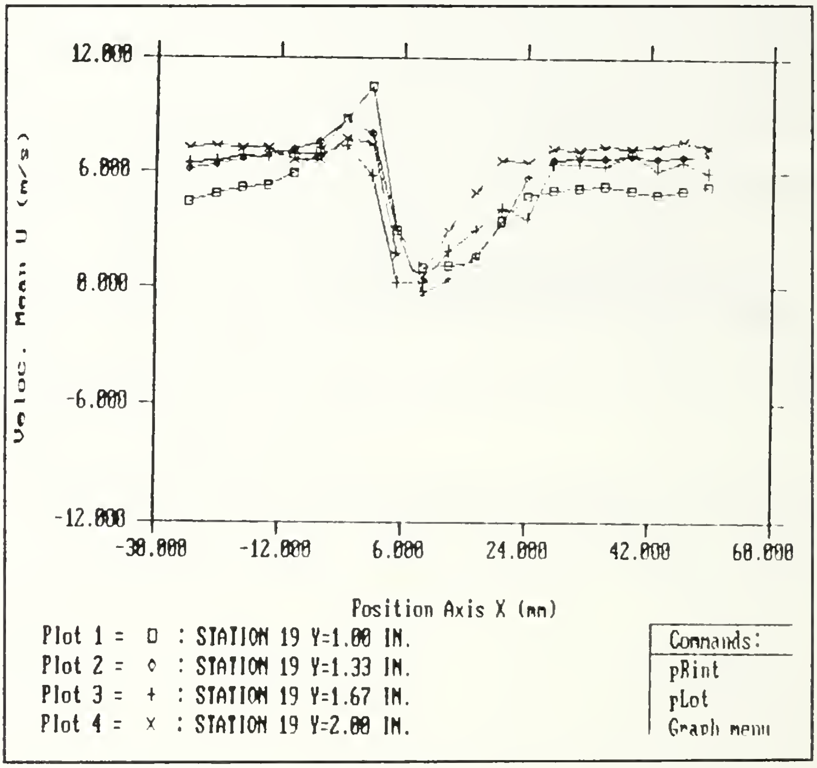

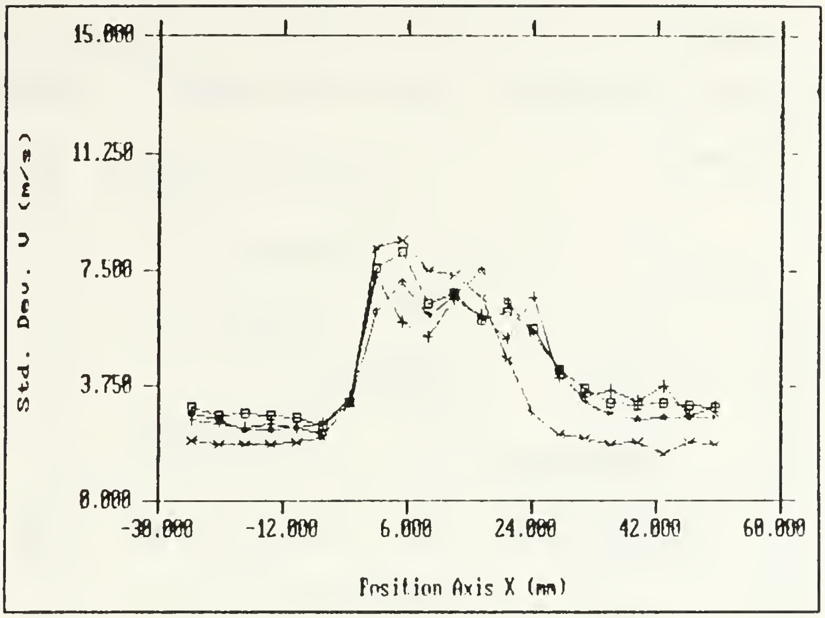
15.000
11.250
7.500
3.750
0.000
-30.000
-12.000
6.000
24.000
42.000
60.000
Std. Dev. U (m/s)
Position Axis X (mm)

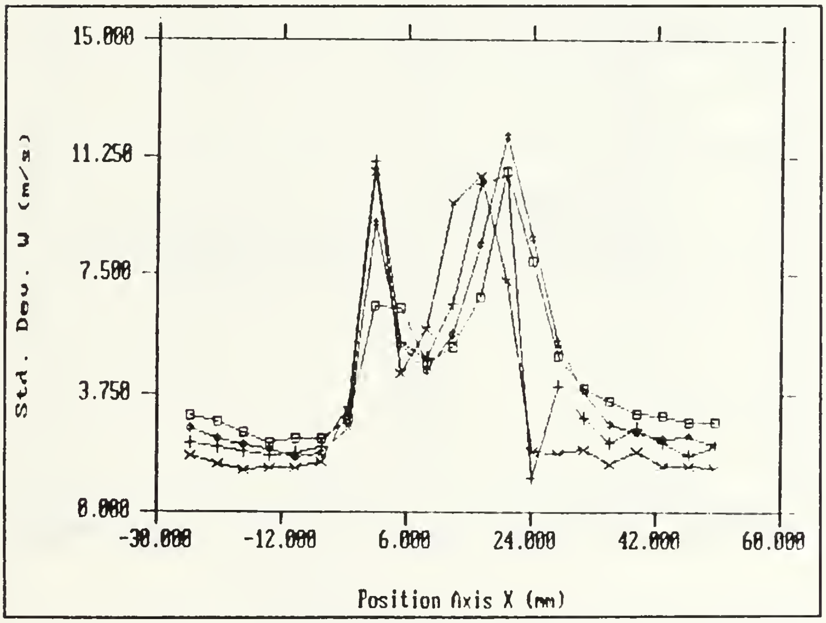
15.000
11.250
7.500
3.750
0.000
-30.000
-12.000
6.000
24.000
42.000
60.000
Std. Dev. W (m/s)
Position Axis X (mm)

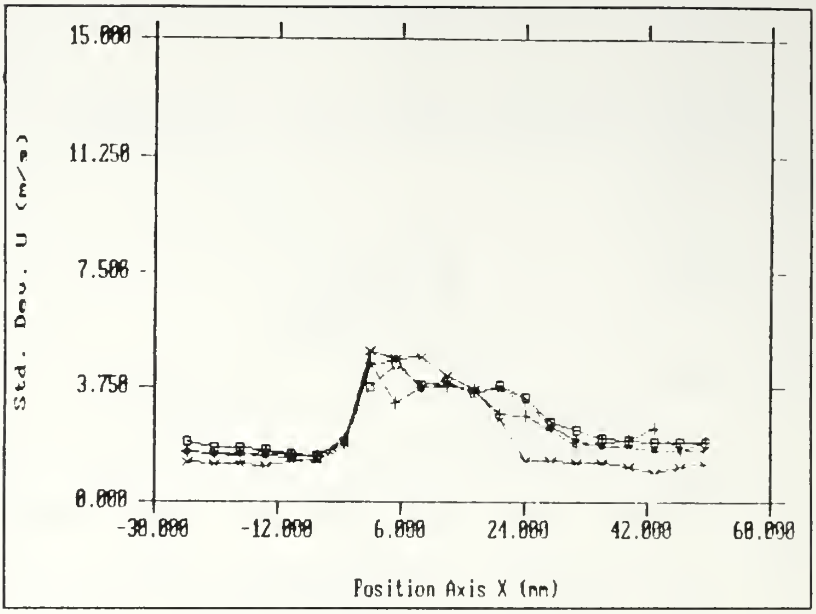
15.000
11.250
7.500
3.750
0.000
-30.000
-12.000
6.000
24.000
42.000
60.000
Std. Dev. U (m/s)
Position Axis X (mm)

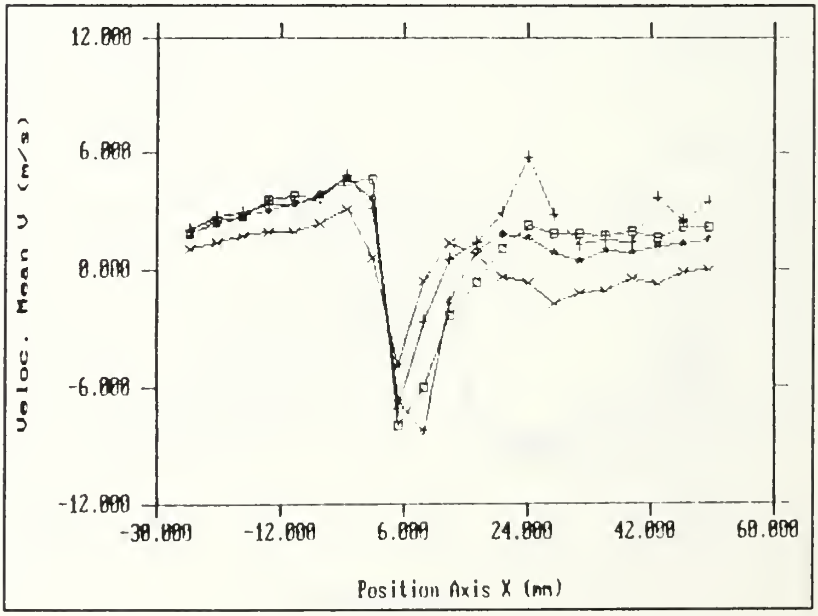
12.000
6.000
0.000
-6.000
-12.000
-30.000
-12.000
6.000
24.000
42.000
60.000
Veloc. Mean U (m/s)
Position Axis X (mm)

APPENDIX C. RAKE PROBE DATA TABULATION, RE_C=240000

A. UPSTREAM SPANWISE SURVEYS

Station 1, 18.5 inches in pitch.

Port Number	C_p
[illegible]	0.1882
[illegible]	0.3126
[illegible]	0.4141
4	0.6154
5	0.8134
6	0.8822
7	0.9265
8	0.9787
12	0.9542
13	0.9607
14	1.0000
15	0.9853
16	0.9133
17	0.7480
18	0.3715
19	0.2193
20	0.1326

Station 2, 19 inches in pitch

Port Number	C_p
1	0.0848
2	0.2365
3	0.4192
4	0.5677
[illegible]	0.7259
6	0.7863
7	0.8091
8	0.8499
12	0.9853
13	0.9804
14	1.0000
15	0.9837
16	0.9380
17	0.7732
18	0.6003
19	0.5383
20	0.4731

Station 3, 19.5 inches in pitch.

Port Number	C_p
1	0.0953
2	0.2676
3	0.4465
4	0.6756
5	0.7876
8	[illegible]
7	0.9064
8	1.0000
12	0.9950
13	0.9532
14	0.9950
15	0.9783
16	0.9164
17	0.5819
18	0.3579
19	0.2943
20	0.2408

Station 4, 20 inches in pitch.

Port Number	C_p
[illegible]	0.0687
[illegible]	0.2345
[illegible]	0.4506
4	0.6767
5	0.8626
6	0.9213
7	0.9631
8	0.9749
12	[illegible]
13	[illegible]
14	1.0000
15	0.9832
16	0.9548
17	0.7136
18	0.4489
19	0.3333
20	0.2513

Station 5, 20.5 inches in pitch.

Port Number	C_p
1	0.0314
[illegible]	0.2926
3	0.2926
4	0.5355
5	0.6942
6	0.7240
7	0.7438
8	0.7537
12	1.0000
13	0.9669
14	0.9950
15	0.9802
16	0.9587
17	0.7967
18	0.4595
19	0.3736
20	0.2760

Station 6, 21 inches in pitch.

Port Number	C_p
1	0.1443
2	0.1611
3	0.3557
4	0.5906
[illegible]	0.7651
6	0.8557
7	0.9084
8	0.9889
12	0.9698
13	0.9664
14	0.9889
15	0.9004
16	0.9161
17	0.7500
18	0.3574
19	0.2182
20	0.1007

Station 7, 21.5 inches in pitch.

Port Number	C_p
1	0.0235
2	0.2114
3	0.3909
4	0.5873
5	0.7651
6	0.8607
7	0.9245
8	0.9933
12	0.9889
13	[illegible]
14	0.9889
15	1.0000
16	0.9111
17	0.8423
18	0.5738
19	0.3842
20	0.2685

Station 8, 22 inches in pitch.

Port Number	C_p
1	0.9890
2	0.9890
3	0.2656
4	0.5018
5	0.7436
6	0.9158
7	0.9890
8	0.9927
12	0.9890
13	0.9890
14	0.9090
15	0.9835
16	0.9579
17	0.8462
18	0.5586
19	0.3773
20	0.2162

Station 9, 22.5 inches in pitch.

Port Number	C_p
1	0.0415
2	0.1711
3	0.3721
4	0.9967
[illegible]	0.7691
6	0.9203
7	0.9967
8	0.9967
12	1.0000
13	0.9635
14	0.9900
15	0.9967
16	0.9518
17	0.8058
18	0.5548
19	0.3439
20	0.2342

Station 10, 23 inches in pitch.

Port Number	C_p
1	0.0245
2	0.2242
3	0.2995
6	0.5270
8	0.7610
6	0.8920
7	0.9329
8	0.9836
12	0.9804
13	1.0000
14	1.0000
15	0.9804
16	0.9116
17	0.7332
18	0.4992
19	0.2979
20	0.2455

Station 11, 23.5 inches in pitch.

Port Number	C_p
1	-0.0049
2	0.1203
3	0.3344
4	0.5750
5	0.7446
5	0.8303
7	0.8995
8	0.9835
12	0.9522
13	0.9539
14	1.0000
16	0.9852
16	0.9160
17	0.7990
18	0.5173
19	0.3328
20	0.2702

B. DOWNSTREAM SPANWISE SURVEYS

Station 1, 18.5 inches in pitch.

Port Number	C_p
1	0.3516
2	0.3880
3	0.4610
4	0.5771
5	0.7711
6	0.7910
7	0.8226
8	1.0000
12	0.9917
13	0.9967
14	0.9386
15	0.8673
16	0.8607
17	0.8590
18	0.8043
19	0.7280
20	0.7181

Station 2, 18.75 inches in pitch.

Port Number	C_p
1	0.2318
2	0.2978
3	0.3892
4	0.4941
5	0.7902
6	0.8731
7	0.9255
5	1.0000
12	0.9865
13	0.9966
14	0.9814
15	0.9865
16	0.9340
17	0.7140
18	0.6074
19	0.5668
20	0.5093

Station 3, 19 inches in pitch.

Port Number	C_p
1	0.2479
2	0.3141
3	0.3854
4	0.4567
5	0.7980
6	0.9168
7	0.9406
8	0.9949
12	0.9660
13	1.0000
14	0.9677
15	0.9864
16	0.9185
17	0.6129
18	0.5025
19	0.4567
20	0.4244

Station 4, 19.25 inches in pitch.

Port Number	C_p
1	0.3222
2	0.4224
3	0.4872
4	0.5442
5	0.7485
6	0.9686
7	0.9528
8	0.9862
12	0.8959
13	0.9607
14	0.9725
15	1.0000
16	0.9607
17	0.6680
18	0.5953
19	0.5580
20	0.4853

Station 5, 19.5 inches in pitch.

Port Number	C_p
[illegible]	0.7673
[illegible]	0.4055
3	0.5323
[illegible]	0.5023
5	0.7350
[illegible]	1.0000
7	0.8571
8	0.8802
12	0.8982
13	0.7880
16	0.8871
15	0.9677
16	0.8687
17	0.5760
18	0.6336
19	0.6106
20	0.5207

Station 6, 19.75 inches in pitch.

Port Number	C_p
12	0.4527
2	0.5802
3	0.7143
4	0.6242
5	0.7626
6	1.0000
7	0.7670
7	0.7780
12	0.8637
13	0.8000
14	0.7692
15	0.9648
16	0.8571
17	0.6923
18	0.8066
19	0.7978
20	0.7187

Station 7, 20 inches in pitch.

Port Number	C_p
1	0.4440
2	0.5620
3	0.6780
4	0.6260
5	0.5880
6	0.7820
7	0.6140
8	0.6500
12	1.0000
13	0.7760
14	0.6300
15	0.7820
16	0.6820
17	0.6160
18	0.7700
19	0.7980
20	0.7300

Station 8, 20.25 inches in pitch.

Port Number	C_p
1	0.4573
2	0.5465
3	0.6831
4	0.7021
[illegible]	0.5655
6	0.5465
7	0.5465
8	0.7192
12	1.0000
13	0.9677
14	0.6793
15	0.6262
16	0.5579
17	0.6300
18	0.7894
19	0.8330
20	0.8065

Station 9, 20.5 inches in pitch.

Port Number	C_p
1	0.4573
2	0.5465
3	0.6831
4	0.7021
5	0.5655
6	0.5465
7	0.5465
8	0.7192
12	1.0000
13	0.9677
14	0.6793
15	0.6262
16	0.5579
17	0.6300
18	0.7894
19	0.8330
20	0.8065

Station 10, 20.75 inches in pitch.

Port Number	C_p
1	0.5580
[illegible]	0.4560
[illegible]	0.5960
4	0.6540
5	0.4860
6	0.3860
7	0.4620
8	[illegible]
1	[illegible]
13	1.0000
5	0.6540
1	0.5140
16	0.4600
17	[illegible]
18	0.7440
19	0.8200
20	0.7460

Station 11, 21 inches in pitch.

Port Number	C_p
[illegible]	0.4276
2	0.5488
3	0.6633
4	0.7458
5	0.9[illegible]99
6	0.6010
7	0.6717
8	0.9680
12	0.9899
13	1.0000
14	0.8333
15	0.7290
16	0.6734
17	0.8215
18	0.8620
19	0.8721
20	0.8485

Station 12, 21.25 inches in pitch.

Port Number	C_p
[illegible]	0.3906
2	0.5185
[illegible]	0.6077
4	0.7323
[illegible]	0.7727
6	0.7609
7	0.7929
8	0.9276
12	1.0000
13	0.9933
14	0.9293
15	0.8502
16	0.8434
17	[illegible]
18	0.8805
19	0.9040
20	0.8434

Station 13, 21.5 inches in pitch.

Port Number	C_p
1	0.3305
2	0.4395
3	0.5111
4	0.6712
5	0.8637
6	0.8501
7	0.9370
8	0.9966
12	0.9744
13	1.0000
14	0.9932
15	0.9710
16	0.9676
17	0.9472
18	0.8910
19	0.8842
20	0.8433

Station 14, 21.75 inches in pitch.

Port Number	C_p
[illegible]	0.2767
2	0.3267
3	0.4183
4	0.5300
5	0.8300
6	0.8967
7	0.9233
8	0.9617
12	0.9783
13	0.9833
14	1.0000
15	0.9900
16	0.9833
17	0.9833
18	0.7450
19	0.7183
20	0.7017

Station 15, 22 inches in pitch.

Port Number	C_p
1	0.2346
[illegible]	0.3099
3	0.3938
4	0.4983
5	0.7945
6	0.9229
7	0.9212
8	0.9589
12	0.9384
13	0.9795
14	1.0000
15	0.9983
16	0.9589
17	0.6524
18	0.5822
19	0.5599
20	0.5223

Station 16, 22.25 inches in pitch.

Port Number	C_p
1	0.2976
2	0.3938
3	0.5209
[illegible]	0.5191
[illegible]	0.7314
6	0.9274
7	0.8566
8	0.9183
12	0.7840
13	0.8675
14	0.9093
15	1.0000
16	0.9437
6	0.7[illegible]4[illegible]
18	0.6933
19	0.6915
20	0.6715

Station 17, 22.5 inches in pitch.

Port Number	C_p
[illegible]	0.3587
[illegible]	0.4850
[illegible]	0.6313
[illegible]	0.5691
5	0.7255
6	0.9198
7	0.8116
8	0.8437
12	0.7295
13	0.7615
14	0.8457
15	1.0000
16	[illegible]
17	0.6333
18	0.6754
19	0.6613
20	0.5972

Station 18, 22.75 inches in pitch.

Port Number	C_p
1	0.4511
2	0.6200
3	0.7022
4	0.6844
5	0.7022
6	0.9333
7	0.7156
8	0.7667
12	0.6467
13	0.7822
14	0.7600
15	0.8600
16	0.8600
17	0.6467
18	0.8044
19	0.8000
20	0.7756

Station 19, 23 inches in pitch.

Port Number	C_p
1	0.4034
2	0.5779
3	0.7036
4	0.6191
5	0.5291
6	0.6698
[illegible]	0.5629
8	0.5872
12	1.0000
13	0.7824
14	0.5891
15	0.7749
16	0.6379
17	0.5141
18	0.7205
19	0.7580
20	0.7505

APPENDIX D. LDV SYSTEM COMPARISON

System comparisons were completed comparing a two-component standard optics system and a three-component fiber-optic system. The standard optics system contains beam expanders and the fiber-optic system does not.

	Stand. Op. Blue	Fiber Op. Green	Stand. Op. Blue	Fiber Op. Blue
Mean Velocity (m/sec)	4.831	4.823	5.017	5.140
Turb. Intensity (%)	9.549	8.969	8.898	8.958

	Stand. Op. Blue	Fiber Op. Violet	Stand. Op. Blue	Fiber Op. Blue
Mean Velocity (m/sec)	4.560	4.824	4.683	4.795
Turb. Intensity (%)	11.546	10.578	11.202	9.482

REFERENCES

1. Dong, Y., Gallimore, S.J. and Hodson, H.P., "Three-Dimensional Flows and Loss Reduction in Axial Compressors," ASME Journal of Turbomachinery, v. 109, pp. 354-361, July 1987.

2. Lasser, R. and Rouleau, W.T., "Measurements of Secondary Flow Within a Cascade of Curved Blades and in the Wake of the Cascade," ASME paper 83-GT-24, 1983.

3. Malak, M.F., Hamed, A. and Tabakoff, W., "Three-Dimensional Flow Field Measurements in a Radial Inflow Turbine Scroll Using LDV," ASME Journal of Turbomachinery, v. 109, pp. 163-169, April 1987.

4. Chesnakas, C.J. and Dancey, C.L., "Three-Component LDA Measurements in an Axial-Flow Compressor," AIAA Journal of Propulsion and Power, v. 6, pp. 474-481, August 1990.

5. Pasin, M. and Tabakoff, W., "Laser Measurements of the Flow Field in a Radial Turbine Rotor," AIAA paper 93-0156 presented at the 31st Aerospace Meeting & Exhibition, Reno, Nevada, January 11-14 1993.

6. Cumpsty, N.A., Compressor Aerodynamics, John Wiley & Sons, pp. 334, 1989.

7. Sanger, N.L. and Shreeve, R.P., "Comparison of Calculated and Experimental Cascade Performance for Controlled Diffusion Compressor Stator Blading," ASME Journal of Turbomachinery, v. 108, pp. 42-50, April 1986.

8. Webber, M., Determining the Effect of Endwall Boundary Layer Suction in a Large Scale Subsonic Compressor Cascade, Master's Thesis, Naval Postgraduate School, Monterey, California, March 1993.

9. Classick, M.A., Off-Design Loss Measurements in a Compressor Cascade, Master's Thesis, Naval Postgraduate School, Monterey, California, September 1989.

10. Chandrasekhara, M.F., unpublished class notes from NPS AE-3802, April-June 1992.

11. Elazar, Y., A Mapping of the Viscous Flow Behavior in a Controlled Diffusion Compressor Cascade Using Laser Doppler Velocimetry and Preliminary Evaluation of Codes for the Prediction of Stall, Ph.D. Dissertation, Naval Postgraduate School, Monterey, California, March 1988.

12. Murray, K.D., Automation and Extension of LDV Measurements of Off-Design Flow in a Subsonic Cascade Wind Tunnel, Master's Thesis, Naval Postgraduate School, Monterey, California, June 1989.

13. Walatka, P.P. and Buning, P.G., PLOT3D User's Manual, NASA Fluid Mechanics Division, 1989.

14. NASA Special Publication SP-36, Aerodynamic Design of Axial Flow Compressors, edited by Irving A. Johnson and Robert A. Bullock, 1965.

15. Hobson, G. and Shreeve, R., "Inlet Turbulence Distortion and Viscous Flow Development in a Controlled-Diffusion Compressor Cascade at Very High Incedence," AIAA paper 91-2004 presented at the 27th Joint Propulsion Conference, Sacramento, California, June 24-26 1991.

INITIAL DISTRIBUTION LIST

		No. Copies
1.	Library, Code 0142 Naval Postgraduate School Monterey, California 93943-5002	2
2.	Defense Technical Information Center Cameron Station Alexandria, Virginia 22304-6145	2
3.	Department Chairman, AA Department of Aeronautics Naval Postgraduate School Monterey, California 93943	1
4.	Garth V. Hobson, Turbopropulsion Laboratory Code AA/Hg Department of Aeronautics Naval Postgraduate School Monterey, California 93943	7
5.	Naval Air Systems Command AIR-536T(Attn: Mr. Paul F. Piscopo) Washington, District of Columbia 20361-5360	1
6.	Naval Air Warfare Center Aircraft Division (Trenton) PE-31(Attn: S. Clouser) 250 Phillips Blvd Princeton Crossroads Trenton, New Jersey 08628-0176	1
7.	David M. Dober 1064 Lakewood Dr. Hanford, California 93230	1